# NUMERICAL STUDY OF LOCAL SITE EFFECTS
# ON THE CHARACTERISTICS OF STRONG GROUND MOTION

## A DISSERTATION

*submitted in partial fulfilment of the*
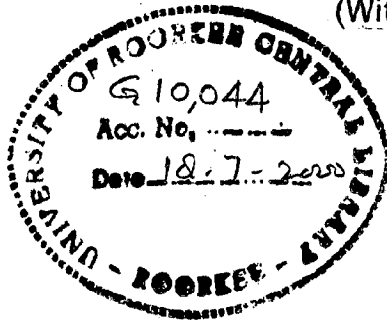*requirements for the award of the degree*
*of*

MASTER OF ENGINEERING

*in*

EARTHQUAKE ENGINEERING

(With Specialization in Soil Dynamics)

*By*

**SANJAY KUMAR MITTAL**

DEPARTMENT OF EARTHQUAKE ENGINEERING
UNIVERSITY OF ROORKEE
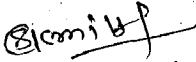ROORKEE-247 667 (INDIA)

MARCH, 1999

# CANDIDATE'S DECLARATION

I hereby declare that the work which is being presented in the dissertation entitled, **"NUMERICAL STUDY OF LOCAL SITE EFFECTS ON THE CHARACTERISTICS OF STRONG GROUND MOTION"**, in partial fulfillment of the requirements for the award of the degree of MASTER OF ENGINEERING in EARTHQUAKE ENGINEERING with specialization in **SOIL DYNAMICS**, submitted in the Department of Earthquake Engineering, University of Roorkee, Roorkee is an authentic record of my own work from July 1998 to March 1999 under the supervision of **Dr. J. P. NARAYAN**, Lecturer, Department of Earthquake Engineering, University of Roorkee, Roorkee, India.

The matter embodied in this dissertation has not been submitted by me for the award of any other degree or diploma.

Place : Roorkee

Dated : March 25, 1999

Sanjay Kumar Mittal

---

This is to certify that the above statement made by the candidate is correct to the best of my knowledge.
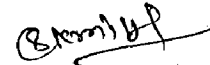
25.3.99

Dr. J. P. NARAYAN
Lecturer,
Department of Earthquake
Engineering,
University of Roorkee,
ROORKEE.

# ACKNOWLEDGEMENT

I wish to express my deep regards and sincere gratitude to *Dr. J.P. Narayan,* Lecturer, Department of Earthquake Engineering, University of Roorkee, Roorkee for his generous help, expert guidance, keen interest, friendly behaviour and continuous encouragement throughout the work.

I also wish to acknowledge the help and encouragement given by all members of the faculty of the Department of Earthquake Engineering and to all my friends who helped me in presenting this dissertation in the present form.

Last but not the least, 1 have no adequate words to express my deep sense of gratitude to my parents who have been a constant source of inspiration.

SANJAY KUMAR MITTAL

# ABSTRACT

The main objective of this dissertation is to study the local site effects on the characteristics of the strong ground motion. Parsimonious staggered grid finite difference method has been used in the computations instead of standard staggered grid scheme since it requires lesser computational memory and enjoys the same advantage of being stable at large poission's ratio and free from the spatial derivative of elastic parameters. Different shear dislocation sources using SH-wave have been generated with the help of partial stress drop in the form of Ricker wavelet and the radiation patterns were found in good agreement with the numerical and analytical radiation patterns. The effects of stress drop, rupture area, slip and time steps on the ground response have been studied for the purpose of numerical source scaling and results were fond in concordance with the different relations developed in the past based on the observed data. The effects of various basin geometry on the characteristic of SGM has been studies in detail and results depect that basin causes amplification in amplitude and duration. These effects are further amplified when basin is narrow and deep. Also, changes in the ground response due to half filled and full - filled reservoir for different source position has been studied.

# CONTENTS

# LIST OF FIGURES

Safe guarding life and property from the destructive effects of earthquakes is a major world wide problem. In spite of the increased awareness of this problem, earthquakes each year claim many lives and cause enormous damage to man-made structures and other facilities. In order to design safe, economical structures and facilities in earthquake prone regions of the world, it is necessary to understand the nature of ground motion that these systems may be expected to experience during their life times. This understanding can ultimately come only from the measurement and subsequent study of strong ground motion resulting from actual earthquakes. The accurate study of characteristics of the strong ground motion (SGM) during large earthquake is of prime importance in Earthquake Engineering. Changes observed in earthquake ground motion from one location to another are the results of several factors such as the source mechanism, the distance and geological characteristics of the rocks from source to site, wave interference and local soil conditions at the site. Analysis of the source mechanism and the effects of transmission path geology on seismic waves is an important area of seismology. The effects of local site conditions on the characteristics of the ground motion have been the focus of research by both seismologists and geotechnical engineers.

Soil parameters and geologic conditions that may have significant effects on the amplification of ground motion at a site include, depth of soil layers above bedrock, variation of soil type and properties with depth, lateral irregularity and surface topography geometry at the site. The predictive modelling of earthquake ground motion requires model simulation of earthquake processes including earthquake mechanism, energy release pattern, seismic wave radiation

and the influence on seismic wave propagation from crustal structure to local soil conditions. The Fig.1.1 schematically shows the factors to be considered in predictive modelling of strong ground motion. Investigation of soil structure interactions based on such realistic ground motion parameters form the necessary base for the analysis and evaluation of the risk for human lives and property, for vulnerability studies with respect to the present conditions and finally long term measures for minimising earthquake damages. The schematic diagram for earthquake risk analysis and evaluation is shown in Fig. 1.2.

The historical references regarding earthquake damage and local site conditions extends back nearly 200 years. Mac Murdo (1824) noted that "building situated on rock were not much affected as those whose foundation did not reach to bottom of the soil" in the 1819 earthquake in Catch India. Mallet (1862) studied on the (1857) Neapolitan earthquake and noted the effects of local geological condition on damage. Wood (1908) and Reid (1910) showed that the intensity of ground shaking in the 1906 San Francisco earthquake was related to local soil and geologic condition. Gutenberg (1927) developed site dependent amplification factors from recordings of Micro earthquakes at sites with different sub surface conditions. In recent years, the availability of strong motion instruments has allowed local site effects to be measured quantitatively.

Recent examples regarding the effect of local site conditions includes, Michoacan ($M_s$ = 8.1) earthquake which caused only moderate damage in vicinity of its epicenter (near the specific coast of Mexico) but caused extensive damage some 400 km away in Mexico city, and damaged caused by the 1989 Loma prieta, California earthquake in the cities of San Francisco and Okland ( U.S. Geological Survey Staff 1990) and recent damage caused by 1997 Jabalpur
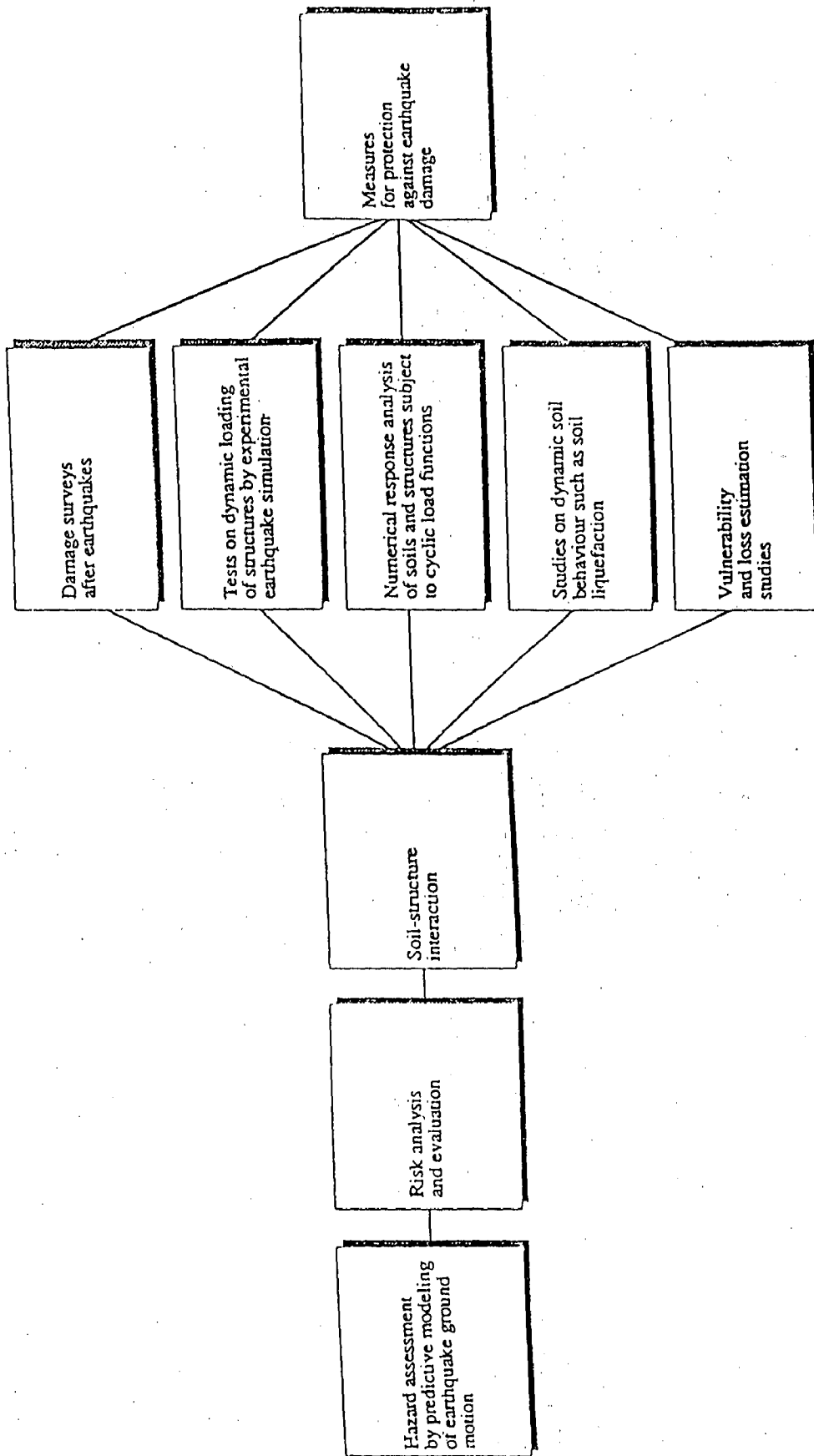
Fig.1.1 Earthquake hazard assessment by predictive modelling of earthquake ground
motion(After, Vogel, and Brandes, 1987).

Measures
for protection
against earthquake
damage

Damage surveys
after earthquakes

Tests on dynamic loading
of structures by experimental
earthquake simulation

Numerical response analysis
of soils and structures subject
to cyclic load functions

Studies on dynamic soil
behaviour such as soil
liquefaction

Vulnerability
and loss estimation
studies

Soil-structure
interaction

Risk analysis
and evaluation

Hazard assessment
by predictive modeling
of earthquake ground
motion

3

Fig.1.2 Earthquake risk analysis and evaluation(After, Vogel, .and Brandes, 1987).

4

Earthquake in India (Rai et al 1997). Studies of ground motions recorded at different sites in Mexico city illustrated the significant relationship between local soil condition and damaging ground motion and led to important advances in understanding the cyclic response of plastic clays Dobry and Vucetic, 1987. In the past, almost most of the seismic simulation works have been done using only explosive source (Virieux, 1984; Kim et.al., 1995; Ram and Narayan, 1995 and Dimitriu et.al., 1998). Numerical implementation of double-couple sources has never been completely presented except Vidale et.al; (1985,87) and Coutant et.al; (1995). Source implementation of Coutant et.al; (1995) is relatively simpler and easier than Vidale et.al; (1985,87) and contains complete source descriptions. The damage pattern in areas having exposed rocks as well as areas underlaid by sediments with varying degree of seismic cross section has been found very complex (Anderson et.al; 1986). The effects of local geology on the characteristics of SGM have been and continue to be a field of active research. In the past, various scientists such as Bard and Bouchon (1980a), Vidale and Helmberger (1987), Hill et.al; (1990), Kim et.al., (1995), and Dimitriu et.al. (1998) have studied its effects numerically.

Strong ground motion is generally associated with earthquakes having magnitude ≥5 or acceleration greater than 0.05g and causing some structural damages to the built invironment. The characteristics of strong ground motion are amplitude, frequency and duration of ground motion. The most common way of describing a ground motion is variation of amplitude (acceleration, velocity and displacement) with time. Frequency is another important parameter in earthquake damage, since building, bridge, slope or soil deposit are very sensitive to frequency at which they are loaded. If frequency of structure and frequency of ground motion coincides then resonance occurs due to this ultimate structure may

5

fall. The most important parameter in earthquake damages is duration. If motion is of short duration, may not produce enough load reversals for damaging response to build up in structure even if amplitude of motion is high. On other hand, a motion with moderate amplitude but long duration can produce enough load reversals to cause substantial damage.

Finite difference method is used to solved the differential equation by replacing temporal and spatial parts using a suitable finite difference operator. In the past a lot of operators have been developed such as second order, fourth order etc. In this thesis parsimonious staggered grid approximation method has been used. Since it required lesser computational memory as compared to standard staggered scheme and is free from spatial derivative of elastic parameters. This scheme is second order accurate in both space and time as well as requires same number of grid points per wave length to avoid dispersion as needed in standard staggered grid scheme.

When slip occurs on the already existing fault, the phenomenon is known as shear dislocation, whereas, when a new fault itself is generated to cause the slip, the phenomenon is known as crack generation. Both these models can be solved by using analytically or numerically. A review of dislocation models, including extensive references has been given by Luco and Andarson (1983). In the dislocation approach the earthquake is represented in terms of slip function on the fault plane. In this thesis Brune's (1970) shear dislocation model is used. In this model it is assumed that a tangential stress drop is applied to the interior of dislocation surface resulting in the fault block movement in the apposite direction. Instead of Brune's instantaneous stress drop a partial

stress drop is applied in the simulation. In contrast to dislocation models, in crack models an explicit account of the deriving and resisting stresses in the source region in taken, and the resulting slip is derived by solving the equation of motion.

## OUT LINE OF THE THESIS

Chapter 2 contains extensive description of finite difference method and various type of shear dislocation source generation. Also, in this chapter effect of slip, stress drop and rupture area on the characteristic of strong ground motion has been studied for the purpose of numerical source scaling.

In chapter 3 we have discussed the effects of basin geometry on the characteristics of SGM. For this purpose different basin geometry has been included in a six horizontal layered model and corresponding numerical responses have been computed.

Chapter 4 contains the description of various types of dams and extensive study of effects of presence of dam as well as variation of water level in reservoir on the characteristics of SGM using different earthquake source positions.

## OBJECTIVE OF THE THESIS

Prediction of ground motion is of prime importance in risk analysis and evaluation of development of measures to prevent damage by future earthquakes particularly in Indian subcontinent due to lack of recorded data. This thesis presents, the simulation procedure and some computed results of SGM by taking into account the earthquake mechanism, energy release, seismic wave radiation, crustal structure and the local site conditions.

## 2.1 SH-WAVE EQUATION

The propagation of a seismic disturbance through a heterogeneous medium is extremely complex. In order to derive equations that describe the propagation adequately, it is necessary to make simplifying assumptions. The heterogeneity of the medium is often modelled by dividing it into parallel layers, in each of which homogeneous conditions are assumed. By suitable choice of the thickness, density and elastic property of each layer, the real conditions can be approximated. The most important assumption about the propagation of a seismic disturbance is that it travels by elastic displacement in the medium. This condition does not apply close to the seismic source. Near an earthquake focus or the explosion the medium is destroyed. The particles of the medium are displaced permanently from their neighbours and the deformation is anelastic. However, when the seismic disturbance has travelled some distance, away from its source its amplitude decreases and the medium deforms elastically to permit its passage.The particles of the medium carry out simple harmonic motion and the seismic energy is transmitted as a complex set of wave motions.

The SH-wave motion is kin to that seen when a rope is shaken horizontal planes moves left and right and adjacent elements of the medium experience shape distortions changing repeatedly from a rectangle to a parallelogram and back. Adjacent elements of medium suffer horizontal shear. So in case of SH-wave, particle motion is in Y direction when wave is moving in X-Z plane.

The 2D dimension SH wave equation in X-Z plane for heterogeneous medium is

$$\rho.\frac{\partial^2 V}{\partial t^2} = \frac{\partial}{\partial x}\left[\mu.\frac{\partial V}{\partial x}\right] + \frac{\partial}{\partial z}\left[\mu.\frac{\partial V}{\partial x}\right] \qquad ...(2.1)$$

Similarly SH-Wave equation for homogeneous medium can be written as

$$\rho.\frac{\partial^2 V}{\partial t^2} = \mu\left[\frac{\partial^2 V}{\partial x^2} + \frac{\partial^2 V}{\partial z^2}\right] \qquad ...(2.2)$$

where,

$\rho$ = Density for the material, and

$\mu$ = Rigidity of the material

V = Particle displacement in Y - direction.

SH-Wave equation in terms of stresses and strains components is written as,

$$\rho.\frac{\partial^2 V}{\partial t^2} = \frac{\partial}{\partial x}\sigma_{xy} + \frac{\partial}{\partial z}.\sigma_{zy} \qquad ...(2.3)$$

Equation (2.3) is an elastodynamic equation for SH-Wave.

$\sigma_{xy}$ = stress in x-y plane

$\sigma_{zy}$ = stress in z-y plane

When we compare equation (2.1) and (2.2) we get

$$\sigma_{xy} = \mu.\frac{\partial V}{\partial x} \text{ and} \qquad ...(2.4a)$$

$$\sigma_{zy} = \mu.\frac{\partial V}{\partial x} \qquad ...(2.4b)$$

## 2.2 PARSIMONIOUS STAGGERED GRID SCHEME

Differencing procedure for SH-Wave equation was developed by Narayan (1998) using parsimonious staggered grid scheme of Luo and Schuster (1990). The

superiority attributed to this scheme is that it is stable for larger range of Poisson's ratio and is free from spatial derivative of elastic parameters over centered difference scheme (Kelly et al., 1976) and lesser storage requirement over the standard staggered grid scheme (Virieux 1984). Stability and grid dispersion criteria for this (2,2) scheme is same as standard staggered grid scheme. Narayan and RAm, 1998). The time derivative in equation 2.3 has been replaced by second order centered difference operator and the body forces have been neglected.

$$\rho_{1,m} \left( \frac{V_{1,m}^{n+1} + V_{1,m}^{n-1} - 2V_{1,m}^{n}}{\Delta t^2} \right) = \frac{\partial}{\partial x} \left( \sigma_{xy} \right)_{1,m}^{n} + \frac{\partial}{\partial z} \left( \sigma_{xy} \right)_{1,m}^{n} \quad ...(2.5)$$

The stresses at time 'n' used in equation (2.5) have been computed using stress-strain relations.

$$\left( \sigma_{xy} \right)_{1,m}^{n} = \mu_{1,m} \left( \frac{\partial V_{1,m}^{n}}{\partial x} \right) = \mu_{1,m} \left[ \frac{V_{1,m}^{n} - V_{1-1,m}^{n}}{\Delta x} \right] \qquad ...(2.6)$$

$$\left( \sigma_{zy} \right)_{1,m}^{n} = \mu_{1,m} \left( \frac{\partial V_{1,m}^{n}}{\partial z} \right) = \mu_{1,m} \left[ \frac{V_{1,m}^{n} - V_{1,m-1}^{n}}{\Delta z} \right] \qquad ...(2.7)$$

The stress approximations has been used as an intermediate terms and need not to be stored. The spatial derivative in equation (2.5) has been approximated using centered difference formula.

$$\rho_{1,m} \left[ \frac{V_{1,m}^{n+1} + V_{1,m}^{n-1} - 2V_{1,m}^{n}}{\Delta t^2} \right] = \left( \frac{\left( \sigma_{xy} \right)_{1+1,m}^{n} - \left( \sigma_{xy} \right)_{1,m}^{n}}{\Delta x} \right) + \left( \frac{\left( \sigma_{zy} \right)_{11,m+1}^{n} - \left( \sigma_{zy} \right)_{1,m}^{n}}{\Delta z} \right)$$

10

Where Δt is time step and Δx and Δz are grid intervals in the X - and Z-directions respectively. 'l' and 'm' are grid indices in the X - and Z-directions and 'n' is the time index.

## 2.3 MODELLING PROCEDURE

While simulating the 2D geological models the grid size (Δx) and the time step (Δt) are fixed to avoid the following constraints.

   (i)    Stability

   (ii)   Grid dispersion

   (iii)  Edge reflection

### 2.3.1 Stability

Every numerical solution which is performed using computer, must be stable. Since instability of the system is owing to the temporal part of the wave equation, hence time step (Δt) is controlled to keep the system stable. Stability condition for the SH-Wave propagation is

$$
\frac{V_{max} \cdot \Delta t}{\Delta x} \leq \frac{1}{2} \qquad \qquad \dots (2.5)
$$

This relation is valid for second order approximation.

where,

$V_{max}$     = Maximum velocity of wave in different concerned layers.

$V_{max} \cdot \Delta t$ = Distance travelled by the wave in time step (Δt)

## 2.3.2 Grid dispersion

Velocity of wave changes with grid size if there are not sufficient number of grids per wave length, according to the order of accuracy. Here, our aim is to avoid grid dispersion. The effect of grid dispersion is to reduce the velocity of higher frequency component. Since grid dispersion is due to the spatial part of the wave equation, hence to avoid grid dispersion, spatial step i.e. grid size ($\Delta x$) is controlled. There should be more than ten grids per wavelength to avoid the numerical grid dispersion for second order accuracy.

## 2.3.3 Edge reflection

Though, edge reflection does not restrict the grid size ($\Delta x$) or time step ($\Delta t$), yet this is an important factor to be considered and requires certain boundary around the edge of the models, so that waves reaching at edge of the model do not reflect back. A composite absorbing boundary condition (combined paraxial wave approximation and the sponge mechanism) has been implemented. This boundary condition is free from the angle of incidence and frequency content in the wave front.

## 2.4 SOURCE GENERATION

In the numerical modelling, we need to generate realistic earthquake source to implement it at the desired co-ordinate of the model. After setting up the source at desired point in grid, we calculate the response at the desired locations. In numerical modelling two type of sources have been used one is point/explosive source, and another is earthquake source. Both the sources can be generated using stress drop in the form of Ricker wavelet is some specified manner. The governing equation to generate a Ricker wavelet is,

12

$$f(t) = C.e^{-\alpha(t-t_0)^2} \qquad \qquad ...(2.10)$$

where

$C$ = A constant whose value is fixed depending on the required amplitude

$t_0$ = Decay time

$\alpha$ = Constants, which control the frequency of the source

The dislocation sources, such as dip slip, strike-slip and explosive have been implemented into the computational grid using Content et al. (1995) method. A dynamic stress drop $\Delta(t)$ in form of Ricker wavelet has been applied to control the frequency content instead of Brune's instantaneous stress drop (1970). Starke-slip, Dip-Slip and explosive sources have been generated by applying the dynamic stress drop in XY- plane, in ZY plane and in both the XY and ZY-planes respectively.

The snapshots at different times for an homogeneous model with rigidity and density as, 10Mpa and 2.5 g/cc have been computed. The dynamic stress drop in the form of Ricker Wavelet with 10Mpa maximum has been used in the computation Fig.2.1a. The radiation patterns computed by Narayan (1998) for the explosive, strike slip and dip-slip cases using SH-Wave have been shown in Fig. 2.1b at two times for same stress drop these radiation patterns are in agreement with the analytical as well as numerical radiation patterns computed by vidale and Helmberger (1985). The radiation patterns computed by Vidale and Helmberger (1985) has been shown in Fig. 2.2 for different source.

## 2.5 SOURCE SCALING

For the purpose of numerical source scaling the effect of stress drop , rupture area, slip and the time step. On the ground response have been studied. In this study SH-wave has been used in computation of responses of various models.

13

Fig. 2.1a Partial stress drop in the form of Ricker wavelet.

Explosion



Strike-Slip

Dip-Slip

(a)                    (b)
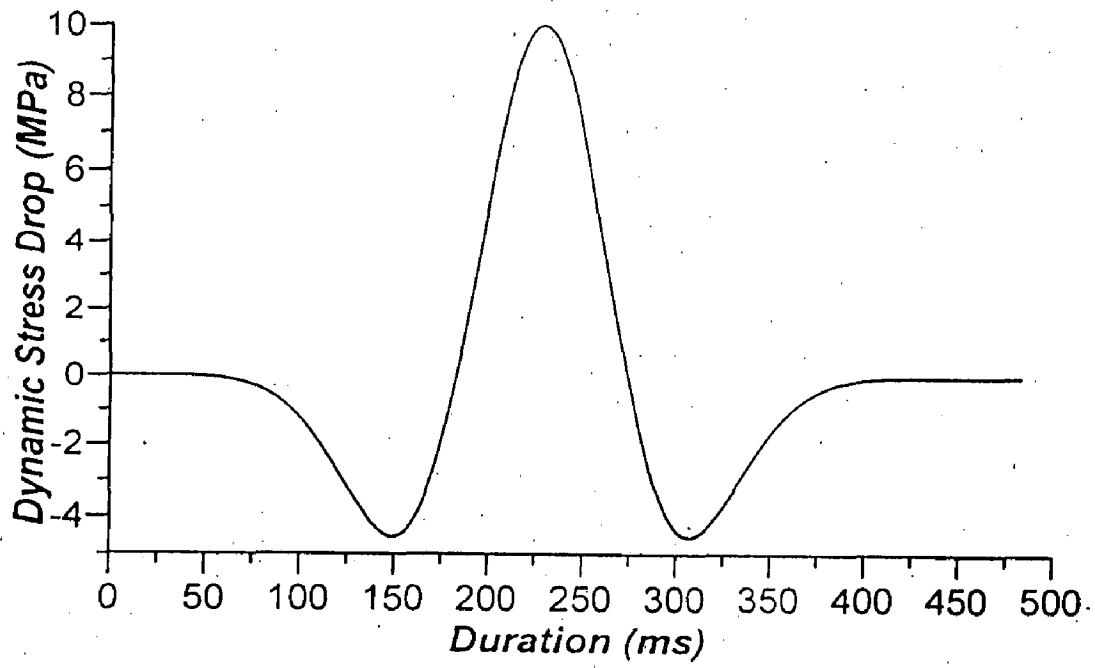
Fig.2.2 Numerical source vertical radiation patterns for SH-wave (After, Vidale, 1985)

Time=60msec                                  Time=100msec



Explosive
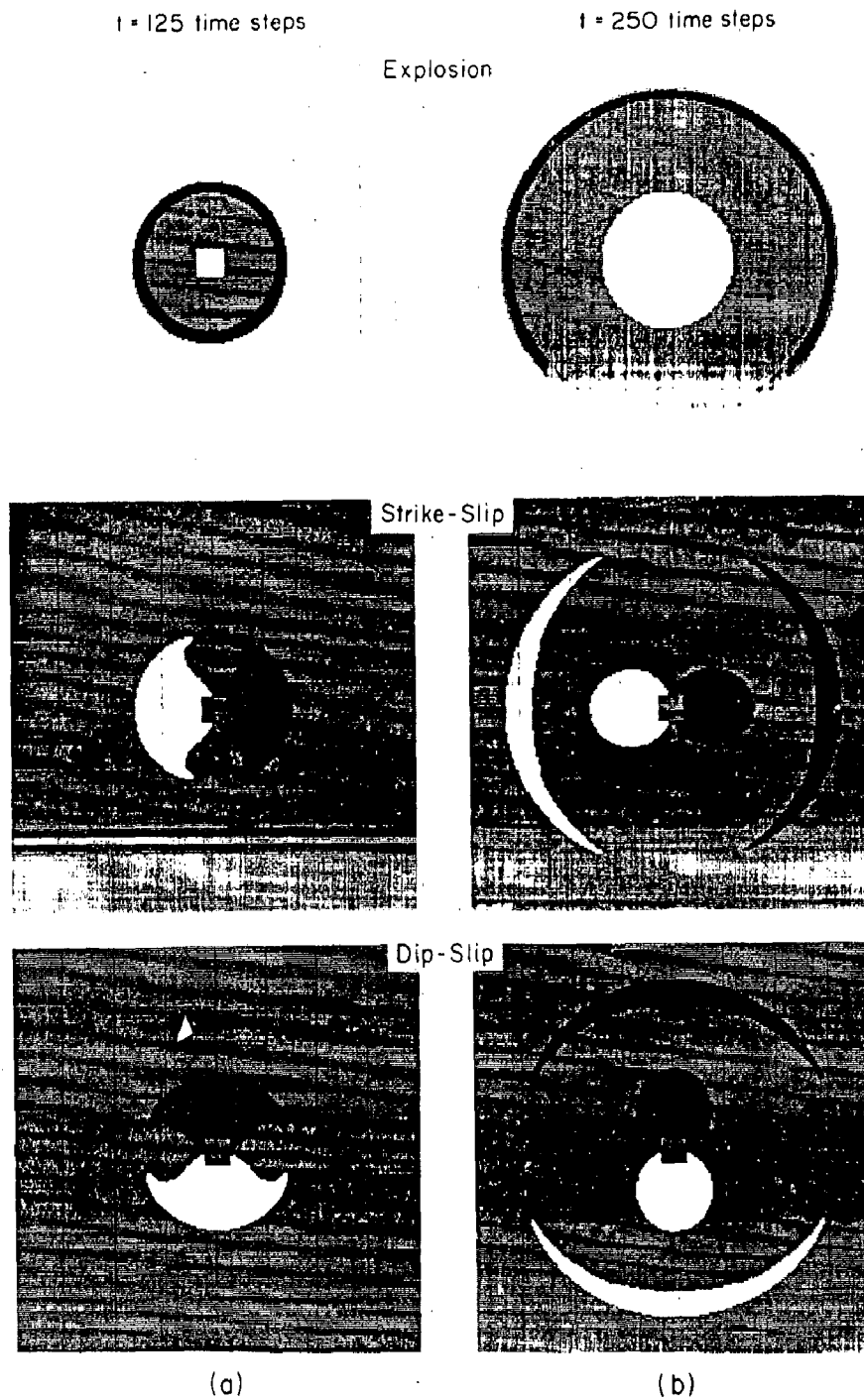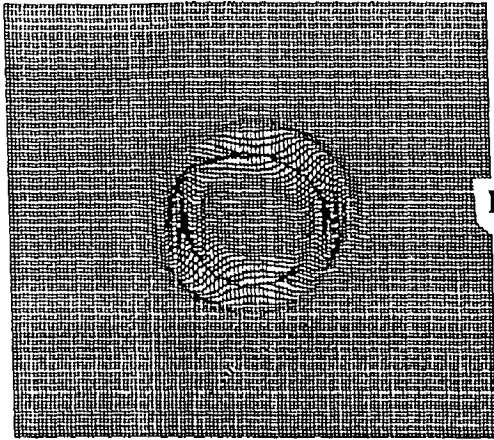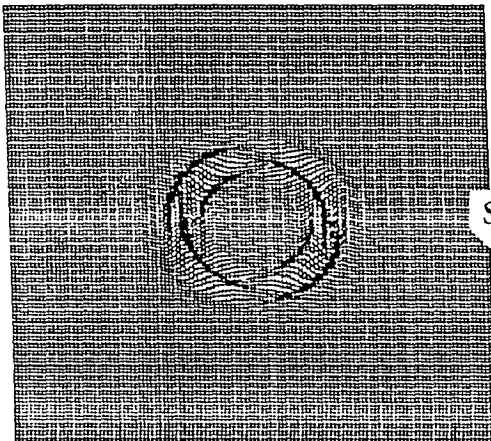(a)
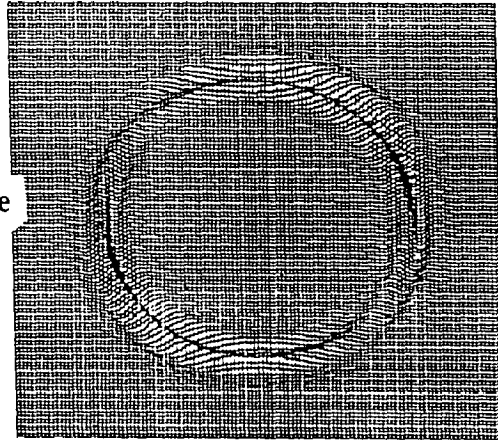
Strike Slip
(b)
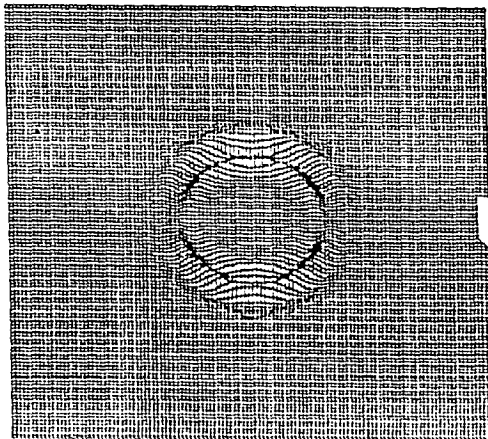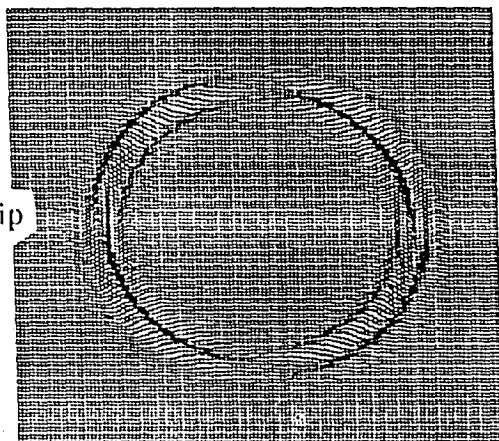
Dip Slip
(c)
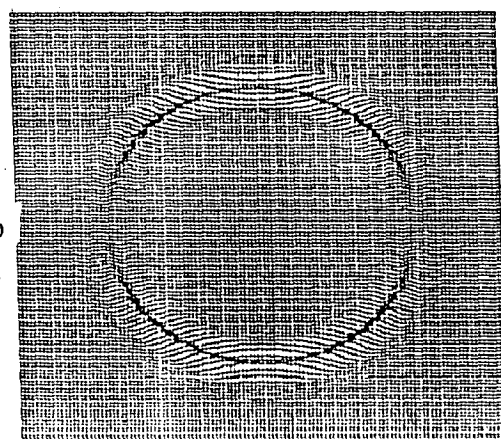
Fig.2.1b Numerical source vertical radiation patterns for SH-wave (After, Narayan,1998)

16

## 2.5.1 Effect of Stress drop

Dynamic stress drop is difference between the original in-situ shear stress and dynamic frictional stress. When a complete stress release is assumed, the stress drop can be calculated from the relation (Brune, .1970).

$$\Delta\sigma = \frac{7}{16} * \frac{M_0}{r_0^3} \qquad \ldots(2.11)$$

where

$M_0$ = Seismic moment

$R_0$ = Radius of circular rupture

$\Delta\sigma$ = Stress drop $(N/m^2)$

And it represent uniform reduction in shear stress effective to produce seismic slip over the circular fault. The stress drop show considerable variability from event to event. Consequently many measures of "stress drop" are reported, but they do not agree with one another for reasons that are difficult to evaluate. For example, one may measure a value of dynamic stress drop averaged over the rupture duration by an interpretation of body wave spectra (Brune, 1970) or from the rms(Root mean square) value of acceleration from strong motion records (Hanks and McGuire 1981), with results that disagree. Evidently, these measurements yield different averages, or are model sensitive in other ways. Some methods determine stress drop over only a part of the rupture event, such as from peak acceleration (Hanks and Johnson, 1976) or slip velocity at the onset of faulting (Boatwright, 1980). As a result, one can not unequivocally quote a "true" stress drop. Various estimates usually agree within only a factor of four or five. This is not error, but an ambiguity in the underlying physics. Within estimates made by a given method one may sensibly discuss relative difference to a finer degree.There are two schools regarding the

dependency of seismic moment on the stress drop. According to first school seismic moment is roughly independent of stress drop (Kanamori and Anderson, 1975., De Matall et. al, 1987., Frankel and Wennerberg, 1989). In contrast to this (Archuleta 1986, Glassmoyer and Borcherdf. 1990, McGarr, 1986) have reported that seismic moment depend upon the stress drop.

The moment magnitude of the earthquake can be calculated using seismic moment (Hanks and Kanamori -1979).

$$M_w = \frac{2}{3} \log_{10} M_o - 6.0 \qquad \qquad ...(2.12)$$

where

$M_o$ = seismic moment

$M_w$ = earthquake magnitude

To study the effect of stress drop/seismic moment on the ground motion as well as to verify the equation (2.12) the response has been computed for different dynamic stress drop. The stresses and corresponding moment magnitudes are given in table 2.1 for fixed circular rupture area. Where rupture area is calculated using the following relation.

$\gamma_o$ = 2.312 x Dominant period x Shear wave velocity

**Table 2.1** Values of stress drop ($\Delta\sigma$), seismic moment ($M_0$) and earthquake magnitude ($M_w$)

| S.No. | $\Delta\sigma$ (N/m$^2$) | $M_0$ (N-m) | $M_w$ |
|-------|--------------------------|-------------|-------|
| 1 | $10.0 \times 10^6$ | $1.800 \times 10^6$ | 4.83 |
| 2 | $10.8 \times 10^6$ | $1.952 \times 10^6$ | 4.86 |
| 3 | $11.6 \times 10^6$ | $2.090 \times 10^6$ | 4.88 |
| 4 | $12.0 \times 10^6$ | $2.169 \times 10^6$ | 4.89 |

**Model specification**

**Model**

| | | |
|---|---|---|
| Type | : | Homogeneous |
| Horizontal extent | : | 3500 m |
| Vertical extent | : | 4000 m |
| Receiver | : | At epicenter |
| Density | : | 2.5 g/cc |
| Rigidity | : | $\mu = 10^7$ N/m$^2$ |
| Shear wave velocity | : | $V_s = 2000$ m/sec |

**Source**

| | | |
|---|---|---|
| Type | : | Dip Slip |
| Focal depth | : | 3500 m at centre of model |
| Frequency | : | 5 Hz |

The desired model has been descritised in to square grid of size 10m. The time step in the simulation is taken as 0.003 second to guarantee the numerical

stability. The partial stress drop in the form of Ricker wavelet was implemented in the model. The response at the epicenter has been computed for a maximum time of 3.0 second. Response has been computed for different value of stress drops given in table 2.1. The output of computations are Particle displacement (cm) and stresses component is XY and ZY planes for different stress drop by using above input value in program. The final results have been shown in Figs 2.3, 2,4 and 2.5 in graphical form. Following facts can be concluded from Fig 2.3.

(i)   The duration of particle displacement is independent of magnitude of stress drop.

(ii)   The amplitude of particle displacement is increasing with stress drop.

(iii)   The arrival time of primary wave is independent of magnitude of stress drop.

Following conclusion can be drawn from Fig 2.4.

(i)   The total duration of stress is independent of the magnitude of applied stress drop.

(ii)   Shear stress at (in XY plane) at the surface is increasing with stress drop.

Following facts can be concluded form this Fig 2.5.

(i)   The amplitude of shear stress (in ZY plane) increases with increasing stress drop.

(ii)   The duration of amplitude of stress is independent of magnitude of applied stress drop.
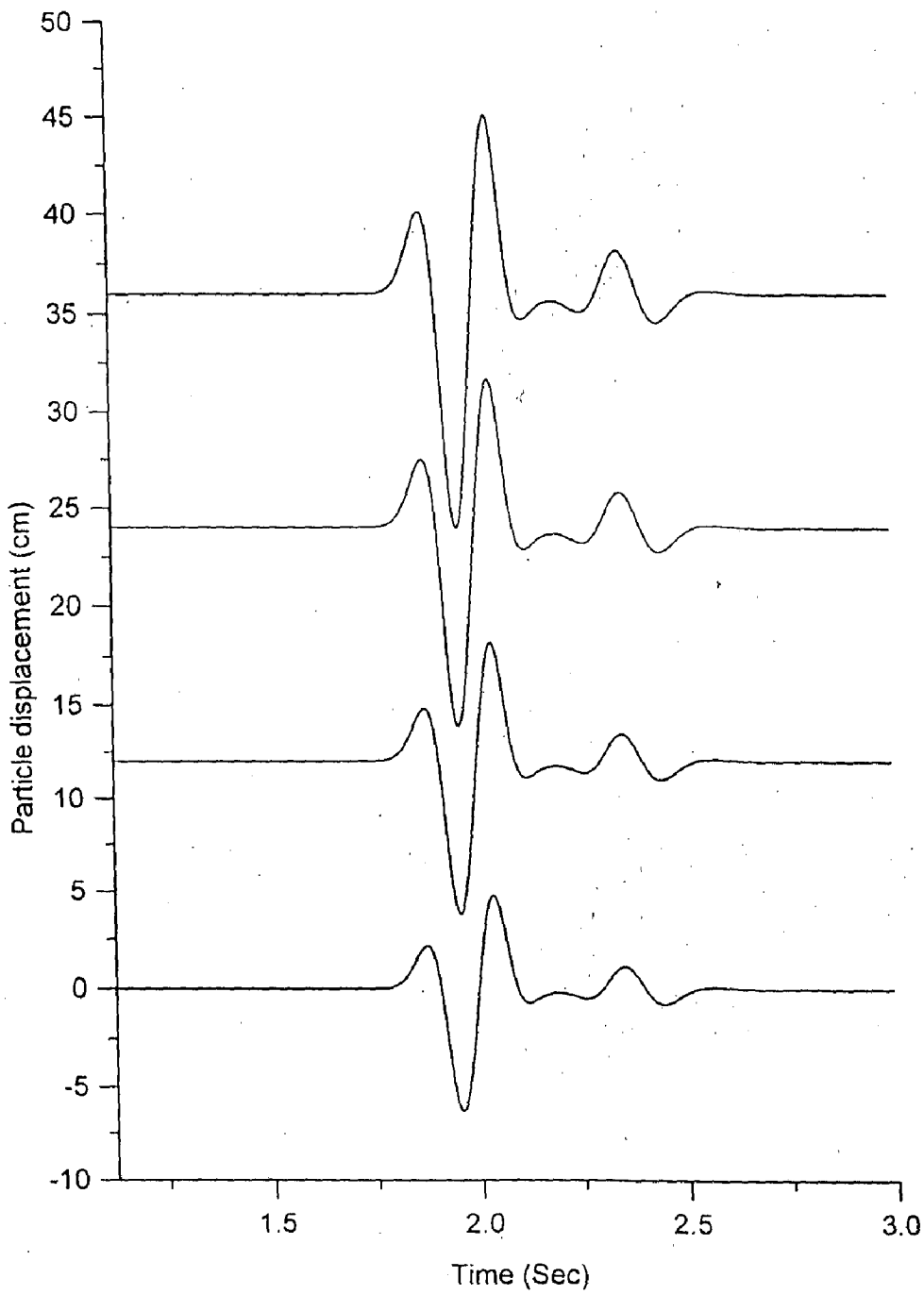
Fig 2.3 Particle displacement for different stress drop using Dip-Slip source
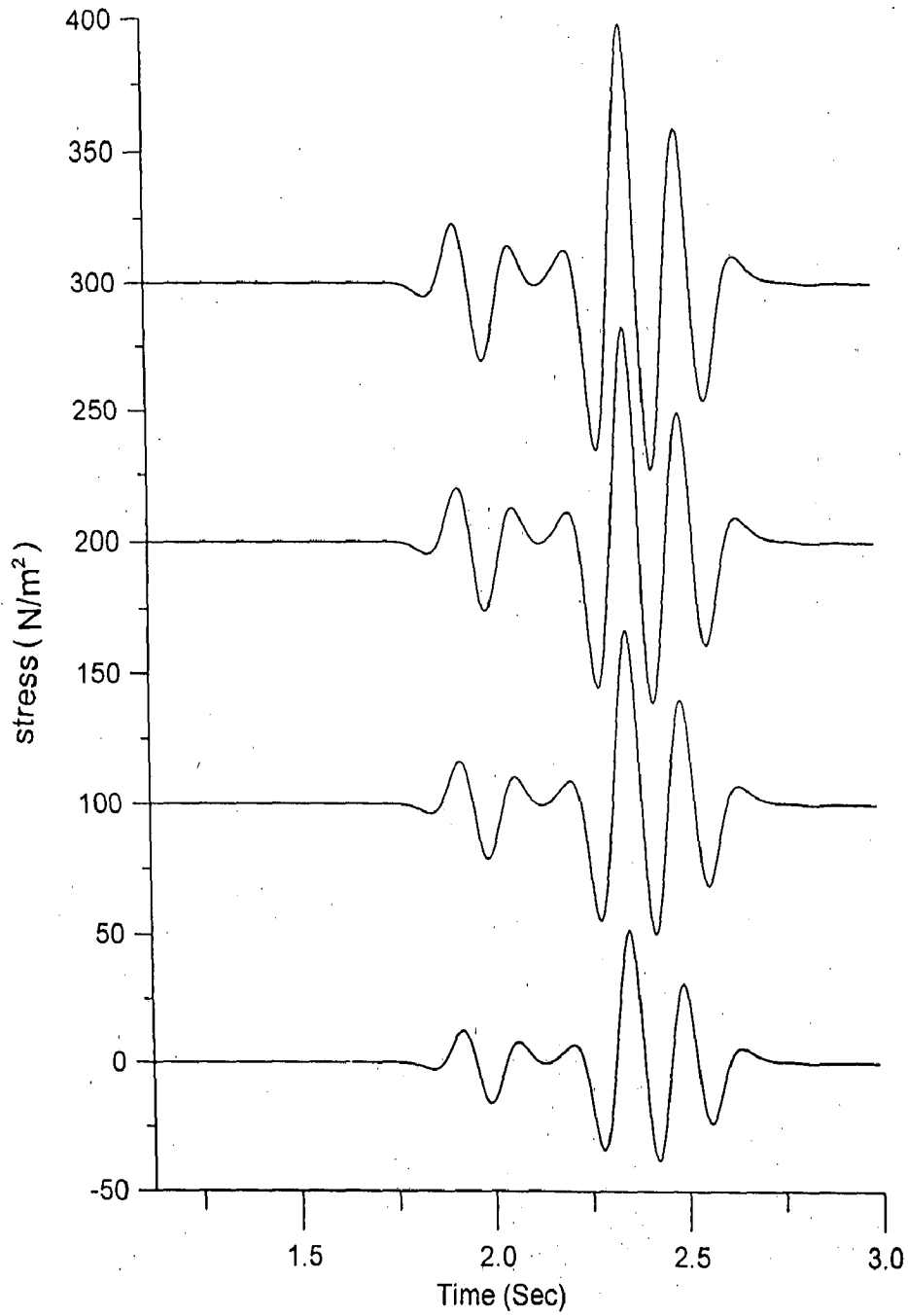
Fig 2.4 Shear stress in XY plane for different stress drop using Dip-Slip source
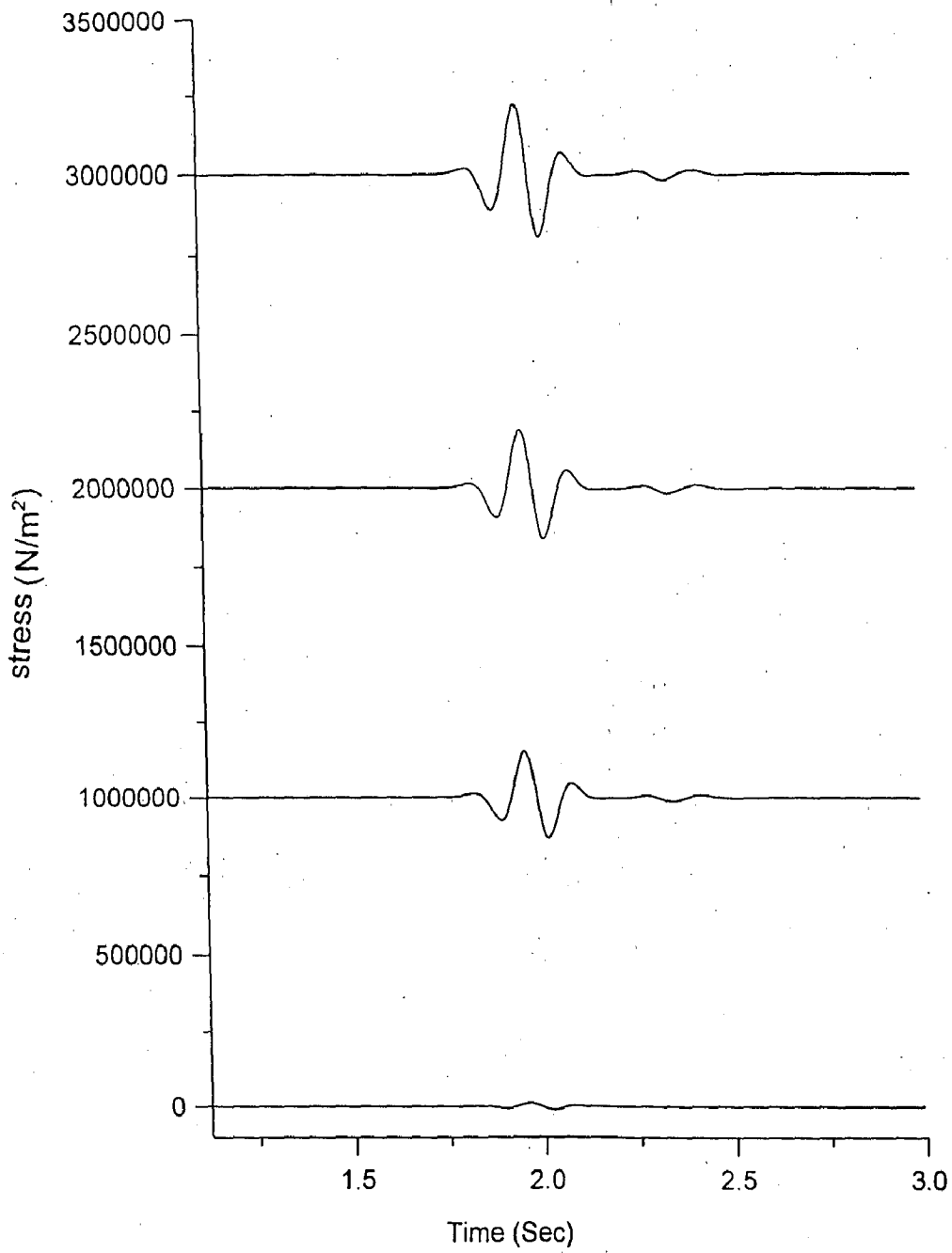
Fig 2.5 Shear stress in ZY plane for different stress drop using Dip-Slip source

## 2.5.2 Effect of Slip

Slip is relative displacement along the interacting faces of fault. Maximum slip, occur near the centre of fault and it taper off to zero at edge . Slip must taper of in such a way that stresses at the crack tip remain finite. To maintain this condition, as slip accumulates a fault will be expected to grow in its lateral dimensions. The fault therefore may be envisioned as having originated at a point, growing with progressive slip and gradually developing its characteristic features. The average displacement ($\bar{U}$) across the fault plane is an important parameter, often in used for the source characterization. The slip ($\bar{U}$) for the circular fault can be calculated directly by the relation given below.

$$\Delta\sigma = \frac{7}{8} * \frac{1}{2.34} * \pi^2 \times \frac{\bar{U} * \mu * f_s}{\beta_0} \qquad \qquad ...(2.13)$$

where,

$\Delta\sigma$ = stress drop = $10^7 N/m^2$

$\bar{U}$ = slip (m)

$\mu$ = rigidity ($N/m^2$)

$f_s$ = dominant frequency of source = 5 Hz

$\beta_0$ = shear wave velocity = 2000 m/s

To study the effect of slip on ground motion as well as to verify the equation 2.13. The slip has been computed for different rigidity and density. Slip is given corresponding to different $\mu$ & $\rho$ in table 2.2 for fixed rupture area.

## Table 2.2

**Value of rigidity ($\mu$), material density ($\rho$) and corresponding slip ($U$)**

| S.No. | Rigidity (M/m$^2$) | Density (g/cc) | Slip (m) |
|-------|--------------------|-----------------|----------|
| 1 | $10.0 \times 10^6$ | 2.5 | 108.38 |
| 2 | $10.8 \times 10^6$ | 2.7 | 100.35 |
| 3 | $11.6 \times 10^6$ | 2.9 | 93.43 |
| 4 | $12.0 \times 10^6$ | 3.0 | 90.32 |

## Model Specification

Type                  : Homogeneous

Horizontal extent     : 1500 m

Vertical extent       : 2000 m

Receiver              : At epicenter

Shear wave velocity   : 2000 m/s

## Source

Type                  : Dip-Slip

Focal depth           : 1500 m

Frequency             : 5 Hz

The desired model has been descritised in to square grid of size 10m. the time step in the simulation is taken 0.002 second to guarantee the numerical stability.    The partial stress drop in the form of Ricker wavelet was implemented in the model. The response at the epicenter has been computed for a maximum time 2 second, Response has been computed for different value slip. The response have been shown in Fig.2.6.

Following facts can be concluded from Fig.2.6.

(i) The amplitude of particle displacement decreases with decrease in slip.

(ii) The duration of particle displacement is independent of the slip.

## 2.5.3 Effect of Rupture Area

We have considered circular rupture area (Brune, 1970) in the modeling. The radius of circular rupture area has been computed using following relation.

$r_o$ = 2.312 x Dominant period x Shear wave velocity

To study the effect of rupture area on the seismic response we have taken different rupture area for the same model parameter using different dominant frequency as shown in table 2.3.

### Table 2.3

**Value of frequency ($f_s$) and corresponding of radius of rupture area**

| $f_s$(Hz) | 5 | 7 | 9 | 11 |
|-----------|-------|--------|---------|--------|
| $r_o$(m)  | 924.8 | 660.57 | 513.786 | 420.36 |

**Specification**

**Model**

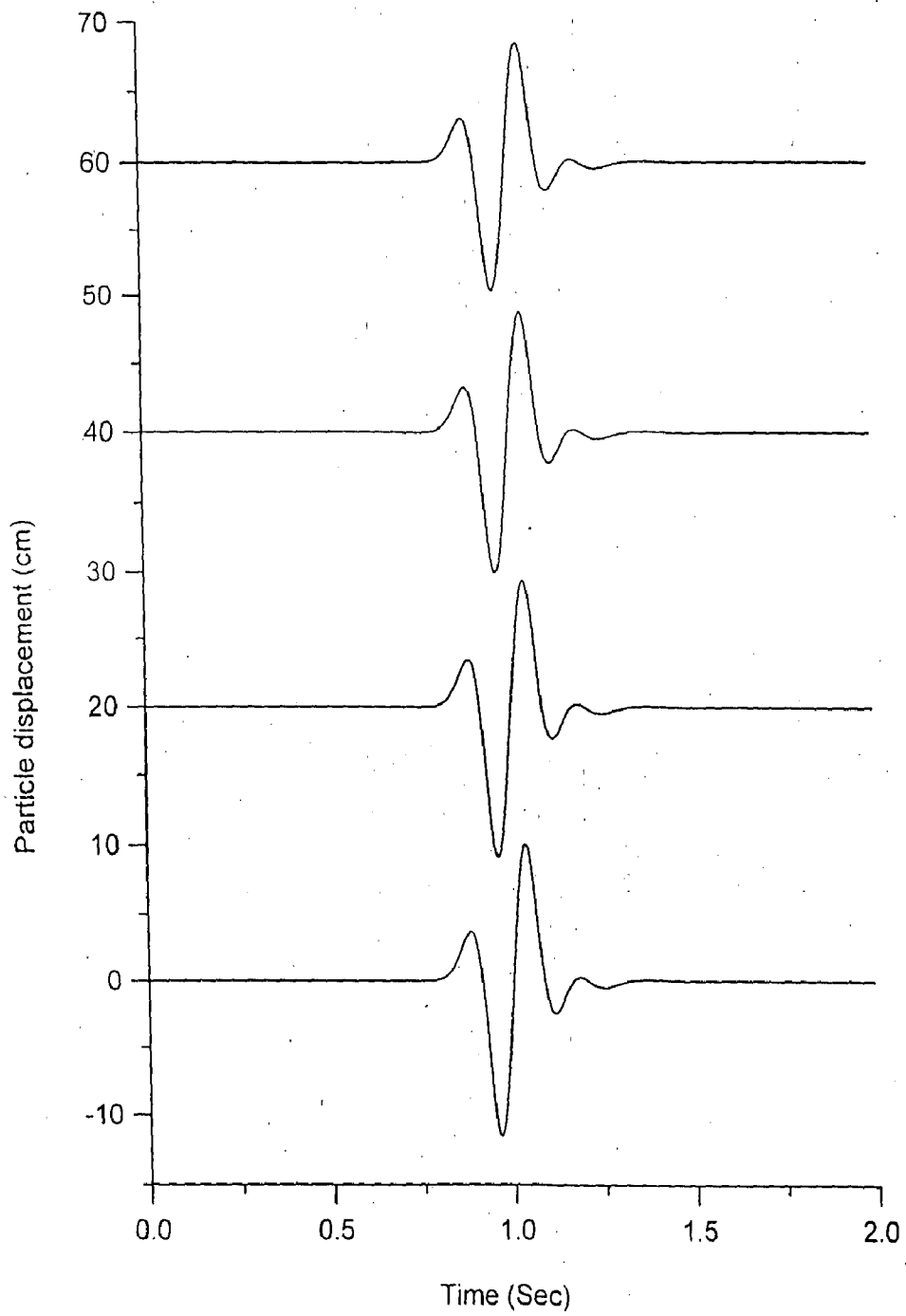| | |
|---|---|
| Type | : Homogeneous |
| Horizontal extent | : 1500 m |
| Vertical extent | : 2000 m |
| Receiver | : At epicenter |
| Shear wave velocity | : $V_s$ = 2000 m/sec |
| Density | : 2.5 g/cc |

26

Fig 2.6 Particle displacement for different slip using Dip-Slip source

27

| Rigidity | : $\mu = 10^7$ N/m$^2$ |
|---|---|

**Source**

| Type | : Dip-Slip |
|---|---|
| Focal depth | : 1500 m at centre of model |
| Maximum stress drop | : $10^7$ N/m$^2$ |

The desired model has been descritised in to square grid of size 10m. The time step in the simulation is taken 0.002 second to guarantee the numerical stability. The partial stress drop in the form of Ricker wavelet was implement in the model. The response at the epicenter has been computed for a maximum time of 2 second. Response has been computed for different rupture area. The response have been shown in Fig.2.7 and following facts can be concluded.

(i)    The amplitude of particle displacement is decreasing with decrease of rupture area.

(ii)   The duration of particle displacement is increasing with the rupture area.

### 2.5.4  Effect of the time step

We have taken different time steps in the simulation to see weather there is any change in the response by increasing or decreasing the number of steps in the stress drop. The computed results have been shown in Fig. 2.8 for the same homogeneous model used in the previous cases with different time steps i.e. 0.003, 0.0025, 0.002s and 0.0015s. The rigidity, density dominant frequency and stress drop used in the simulation are $10^7$ 2.5 5 Hz and 10Mpa respectively. It has been concluded that particle displacement and duration are independent of time steps taken in the computations.
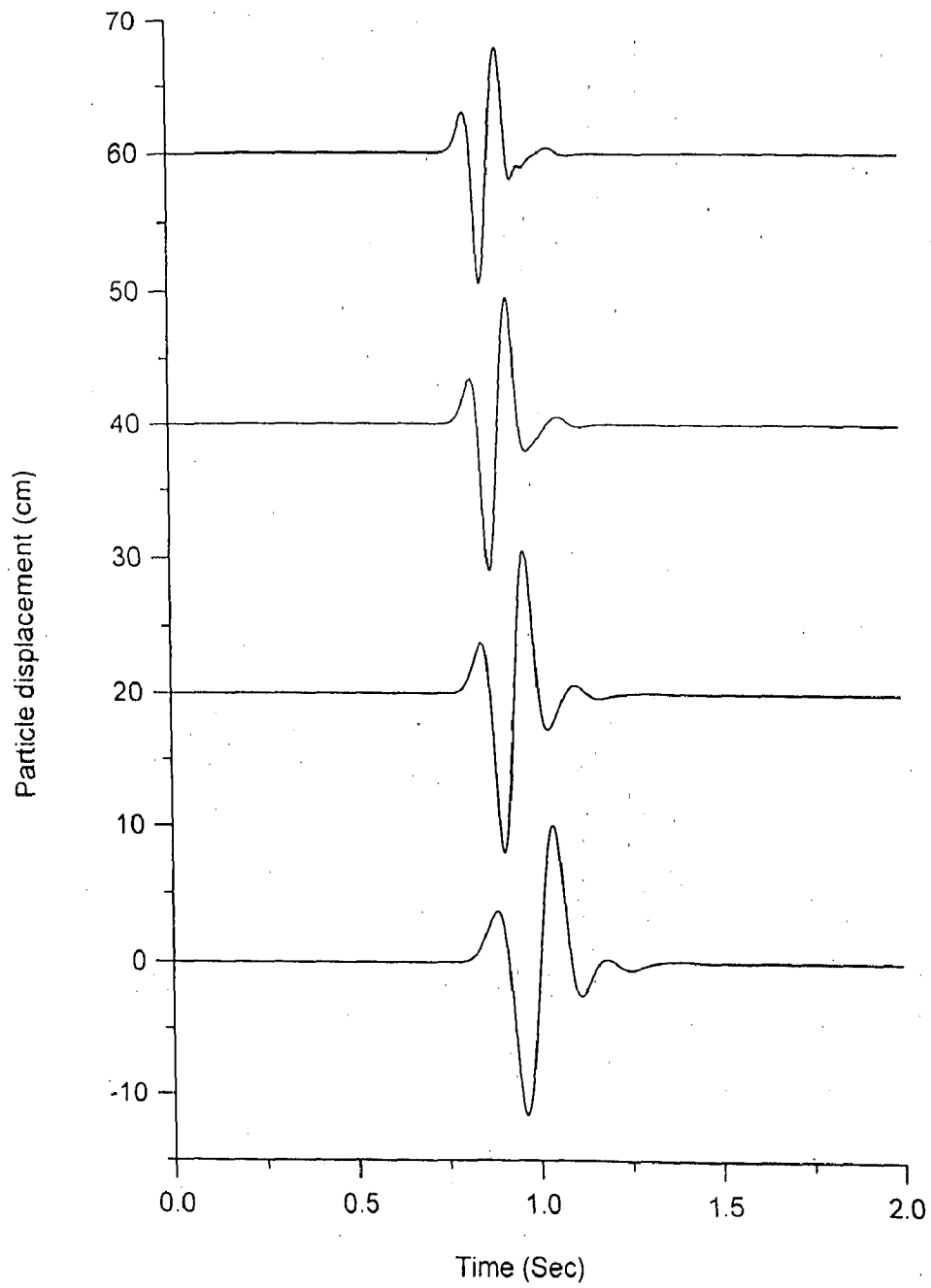
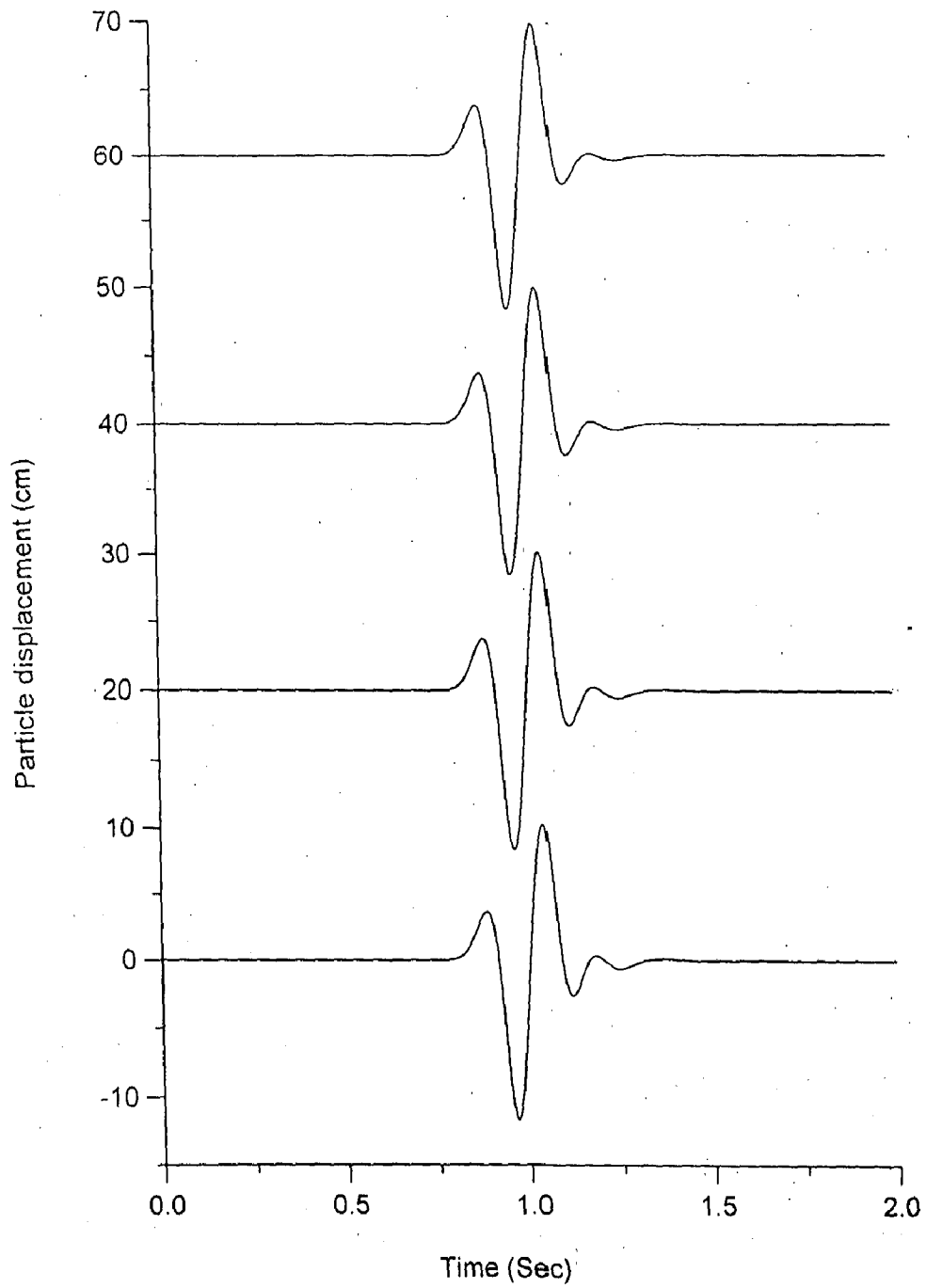Fig 2.7 Particle displacement for different rupture area using Dip-Slip source

Fig 2.8 Particle displacement for different time steps using Dip-Slip source

## 3.1 GENERAL

In this chapter, we have discussed the effects of basin geometry on the characteristics of the strong ground motion. Since many large cities are located on or near alluvial valleys, so the effects of basin geometry on the ground motion is of greater interest in geotechnical earthquake engineering. The curvature of a basin in which softer alluvial soils have been deposited can trap body waves and cause some incident body waves to propagate through the alluvium as surface waves (Vidale and Helmberger, 1988). These waves can produce stronger shaking and longer duration than would be predicted by one dimensional analyses that considers only vertically propagating S-waves. At most sites the density and S-wave velocity of materials near the surface are smaller than at greater depths. If the effects of scattering and material damping are neglected, the conservation of elastic wave energy requires that the flow of energy flux $(\rho V_s \dot{U}^2)$ from depth to the ground surface be constant. Therefore, since $\rho$ and $V_s$ decrease as waves approach the ground surface, the particle velocity $(\dot{U})$, must increase. Due to this reason the amplification takes place.

King and Tucker (1984) measured ground motion along transverse and longitudinal profiles across the Chusal valley near the Afghanistan border of the former Soviet Union. Interpretation of response in a series of small $(M_L \leq 4.0)$ earthquakes he suggested that one dimensional ground response analyses could predict the average response of sediments near the centre of the valley but not at edges. It is discussed later. Significant difference between the

amplification factor at the centre and edges of the valley were observed. Similar effects have been observed for other valleys (e.g., Caracas in 1967, San Fernando in 1971, and Leninakan, Armenia in 1988) in different earthquakes.

## 3.2 SIMULATION OF DIFFERENT BASIN GEOMETRY

The characteristics of earthquake shaking at a given site during a particular event depends on a number of factors, such as the source mechanism, energy released the distance and geological characteristics of rocks from source to site, wave interference and local soil conditions at the site. Analysis of the source mechanism and the effects of transmission path on the earthquake waves is an important area of seismology. The effects of local site conditions on the characteristics of ground motions have been the focus of research by both seismologists and geotechnical engineers. Soil parameters and geologic condition that may have significant effects on the amplification of ground motion at a site include the depth of soil layers bed rock, variation of soil type and properties with depth, lateral heterogeneity surface topography and geometry of basin at site.

Here we have studied effects of various basin geometry on the characteristics of strong ground motion in detail using SH-wave.

### 3.2.1 Specifications of models

We have used four models of basin which are trapezoidal in shape. These four basins are named as narrow and shallow basin (NSB), narrow and deep basin (NDB), wide and shallow basin (WSB) and wide and deep basin (WDB) basins. Figure (1.1) shows geometry of these basins. Nomenclature of these basins has been done based on their relative areal extent and depth.
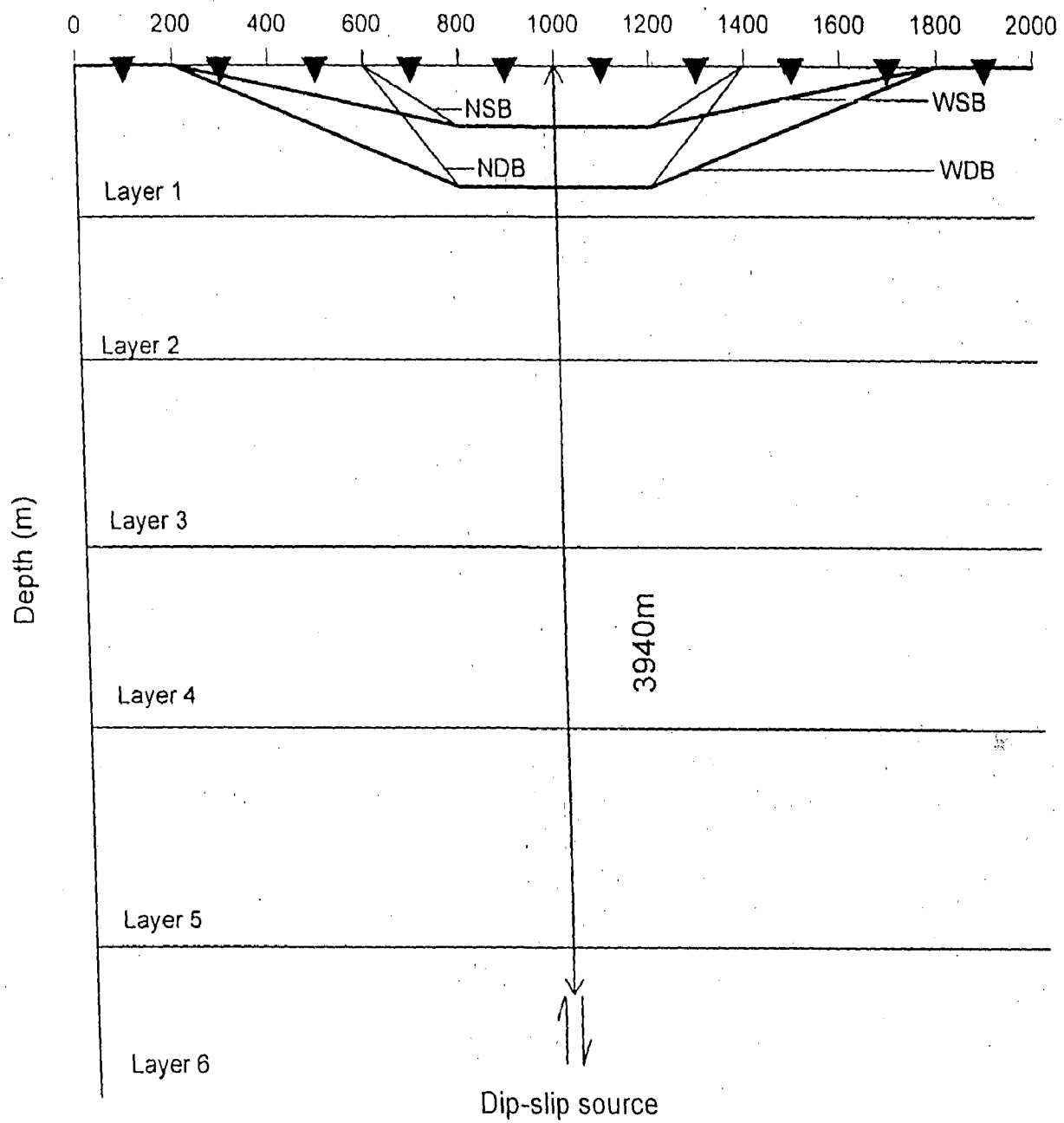
Fig. 3.1 Model geometry of basins.

In each basin simulation, the position of source is just below the centre of the basin, at depth of 3940 m from the free surface. We have taken six layered model having different material property and thickness in which all the four basin have been included. The layer thickness, material density, shear wave velocity, and rigidity of different layer's are given in Table 3.1. The depth of shallow basins is 80m and that of deep basins is 160m. Similarly, the areal extent of narrow basins is 800m and that of wide basin is 1600m. The base of all the basin is 400m wide. In each model simulation, response has been computed at ten equidistant receivers (200 m). The first receiver is placed at 200 m offset from left boundary of the model. The following computational parameters have been taken in the simulations. These model parameters fulfill the requirements to make the simulation stable and dispersion free.

**Model Parameter**

| | |
|---|---|
| Grid Size | : 10 x 10 m |
| Model Size in term of grid | : 280(H) x 450 (V) grid |
| Time step | : 0.002 second |
| Maximum time | : 7 second |
| Total number of time step | : 3500 |
| Dominant frequency | : 4 Hz |
| Type of source | : Dip-slip |

The computer program has been modified according to the different basin geometries. The model parameters listed in Table 3.1 have been assigned to each grid point. The dip-slip source, based on partial stress drop has been implemented into the computational grid at depth of 3940 m below the centre of spread. An observing boundary has been implemented to avoid edge reflections on

Table 3.1 Layer Parameters of the Geological Model Excluding Basin

| S.NO. | LAYER NUMBER | THICKNESS (M) | MATERIAL DENSITY ($\rho$) (G/CC) | SHEAR WAVE VELOCITY ($V_S$) (M/S) | RIGIDITY $\mu$(N/M$^2$) |
|---|---|---|---|---|---|
| 1 | BASIN | VARIABLE | 1.7 | 500 | 425000 |
| 2 | LAYER I | 200 | 2.00 | 1000 | $2.0 \times 10^6$ |
| 3 | LAYER II | 200 | 2.20 | 1200 | $3.168 \times 10^6$ |
| 4 | LAYER III | 630 | 2.30 | 1400 | $4.508 \times 10^6$ |
| 5 | LAYER IV | 670 | 2.40 | 1900 | $8.664 \times 10^6$ |
| 6 | LAYER V | 1300 | 2.50 | 2500 | $15.63 \times 10^6$ |
| 7 | LAYER VI | ---- | 2.60 | 2598.07 | $17.55 \times 10^6$ |

the edges of the model. We get the particle displacement registered by the ten receivers after running the computer program. The response of the six layered model excluding basin has been shown in Fig. 3.2. This Figure depicts the primary arival and different multiples at different times very clearly according to model geometry and the position of the source. Similarly, the responses of all the four basins, namely NSB, NDB, WSB and WDB have been shown in Figures 3.3, 3.4, 3.5 and 3.6 respectively.

## 3.3 EXPLANATION OF COMPUTED RESULTS

(1)  The receivers which were kept at the deepest points of NSB and NDB basins have maximum amplitude in comparison to six receivers which were outside the basins (Figs. 3.3 & 3.4)..

(2)  In case of NDB, there is further amplification of amplitude and duration at deepest points of the basin. This may be due to the focusing effect caused by increased curvature of basin.

(3)  In case of NSB as well as NDB receiver No. (4) and (7) have same distance from source, but more amplitude is recorded by receiver No.

(4)  In case of NSB and NDB, as we move away from the centre of basin towards any one of the edges of basins, the maximum amplitude is decreasing.

(5)  In all four cases there is not much effect on response of receivers placed at the edges of the basin due to increase in thickness.

(6)  In all four cases large duration of signal is due to generation of multiples within basin.

(7)  The responses of WSB and WDB shown in Fig. 3.5 & 3.6 depict smaller amplitude amplification but large signal duration at deepest points of basins as compared to the responses of NSB and NDB.
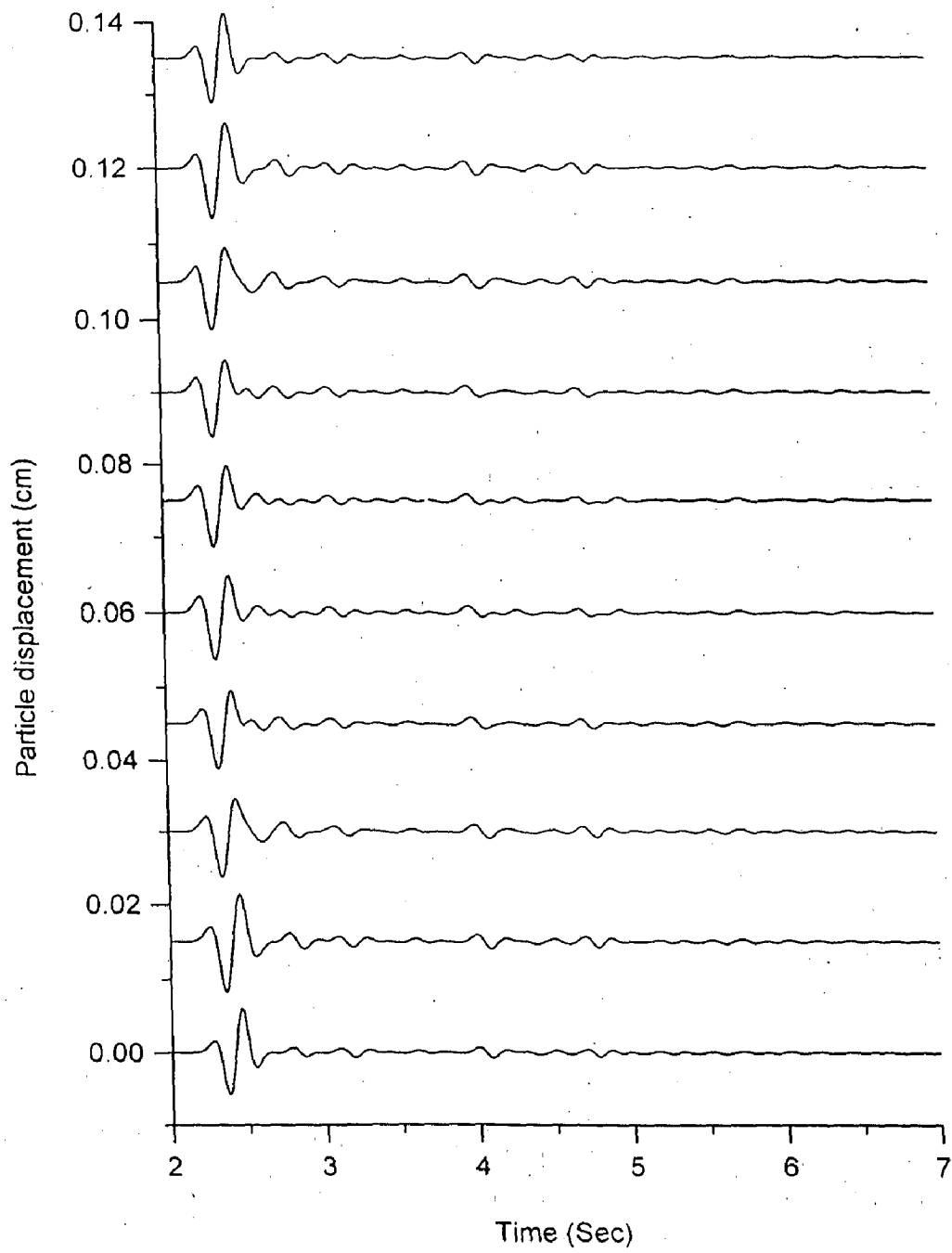
36

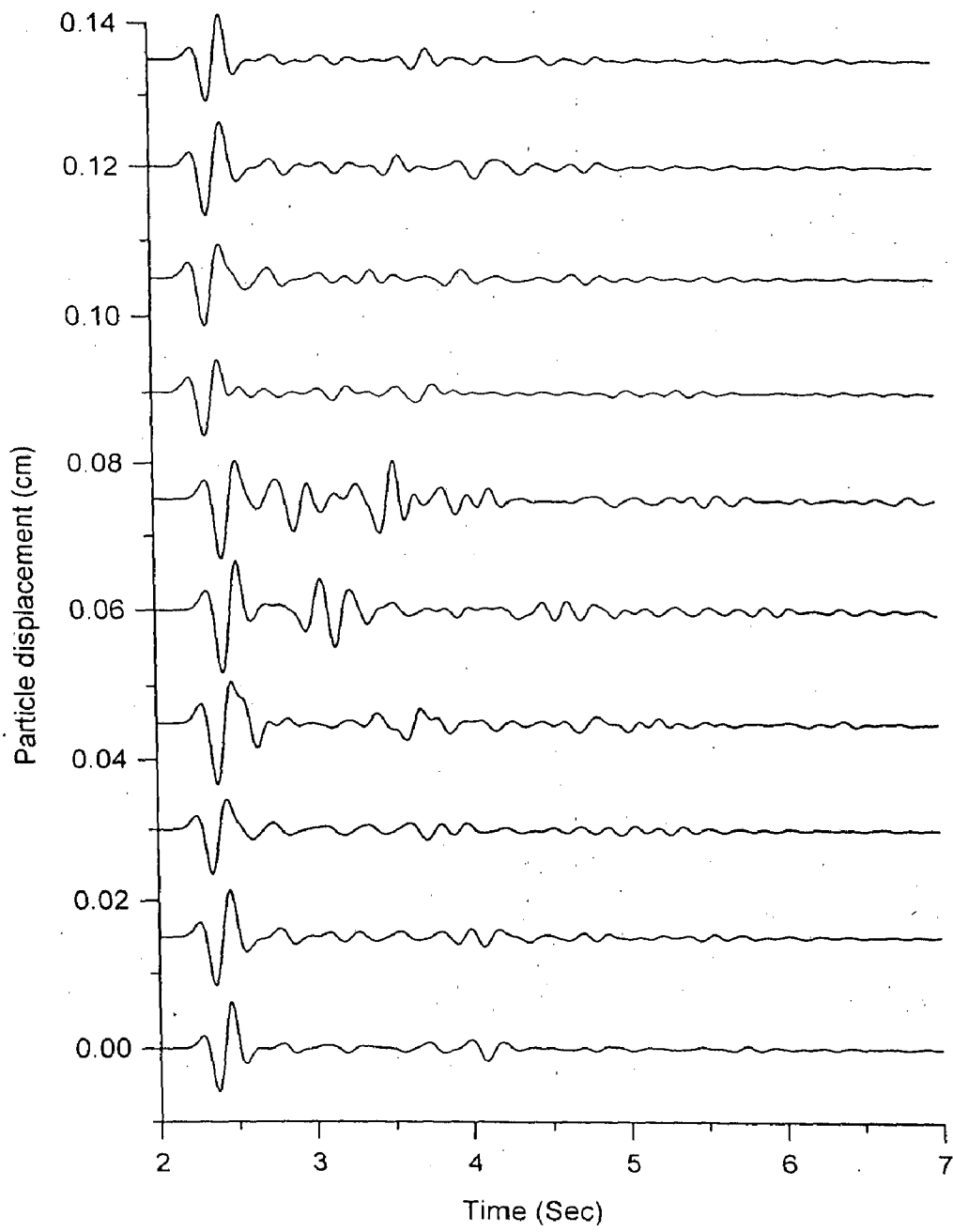Fig 3.2 Response of six layer model excluding basin.

Fig 3.3 Particle displacement at different receivers for NSB.
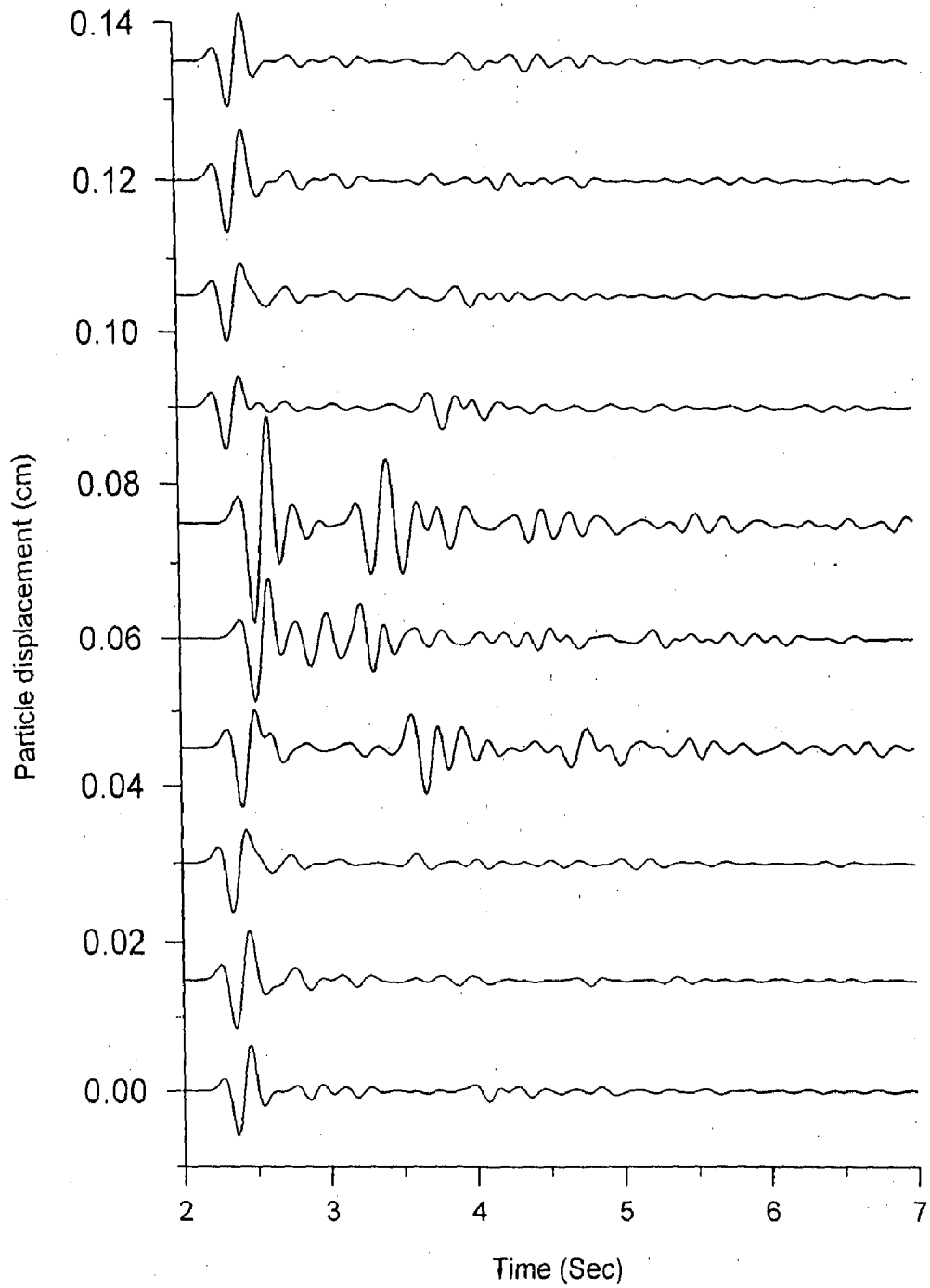
Fig 3.4 Particle displacement at different receivers for NDB.
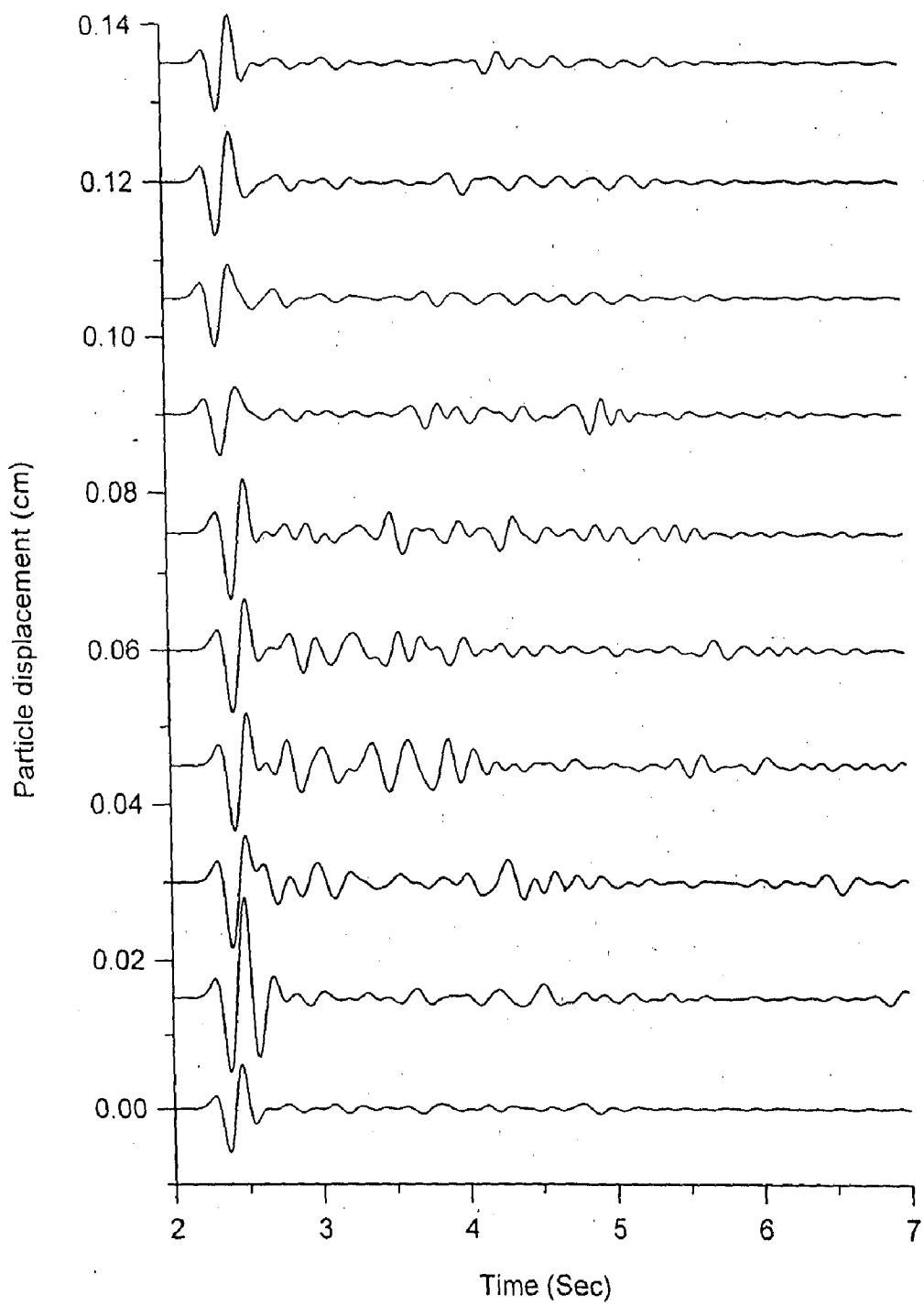
Fig 3.5 Particle displacement at different receivers for WSB.
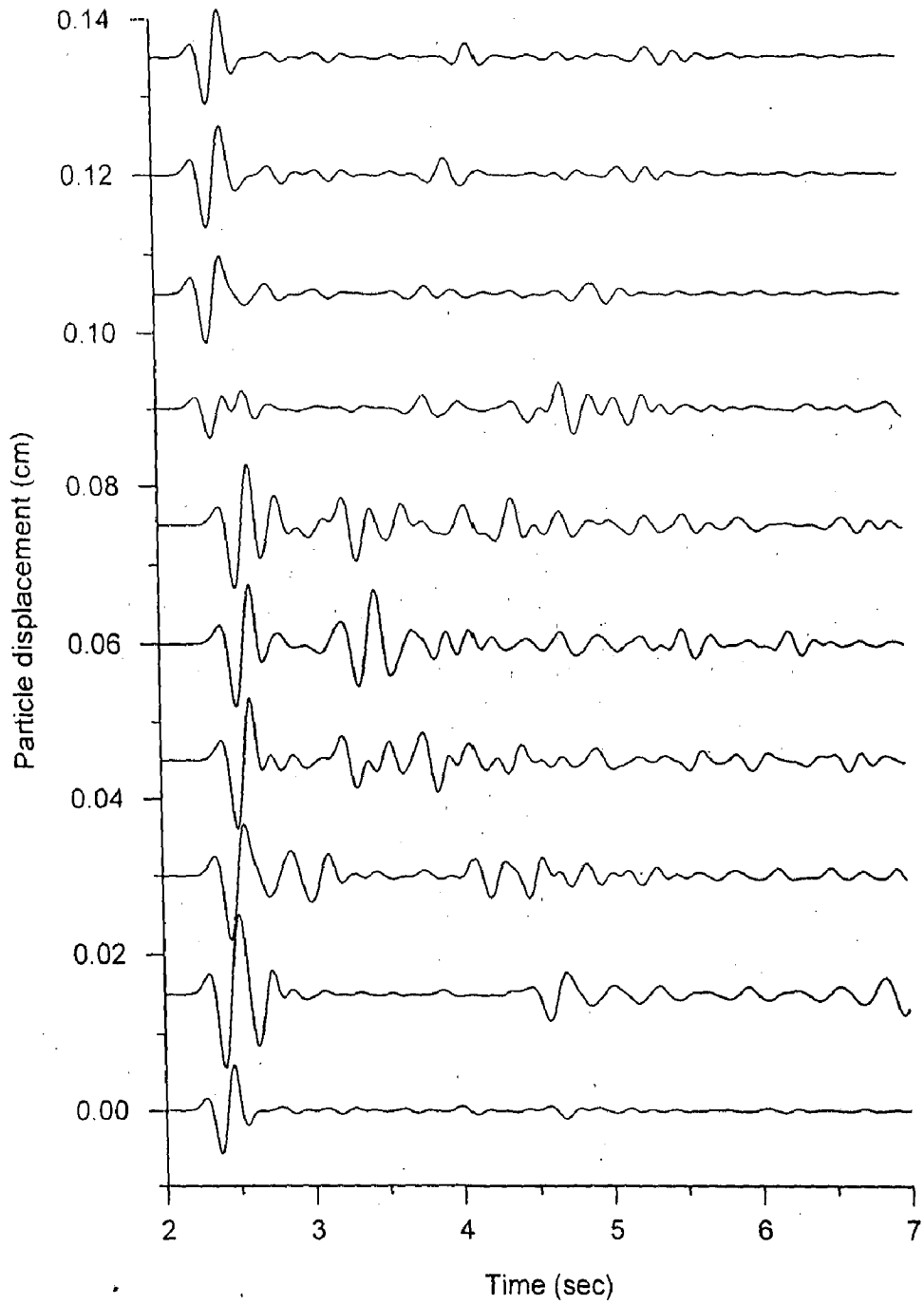
Fig. 3.6 Particle displacement at different receivers for WDB.

41

(8)    Response of WDB reveals more amplitude amplification and signal duration at the deepest points compared to WSB due to larger curvature.

(9)    In case of WSB and WDB receiver No. 2 recorded more amplitude and duration in comparison to receiver No. 9 although distance from source is same.

(10)   Maximum duration is recorded by NDB basin.

(11)   In case of WDB receiver No. 7 recorded much lesser amplitude in comparison to other receiver.

The simulated results of a layered geological model included with and without different basin geometry revals that thicker the basin more will be duration of the signal and lesser the shear strength of basin more will be amplitude amplification. Also, narrow and deeper the basin, the amplitude and duration will be further amplified due to the focusing effect. There effects are more pronounced at the deepest point of the basin.

## 4.1 GENERAL

A dam is a hydraulic structure constructed across a river to store water on its upstream side. Construction of large dam is dictated by the needs at modern day society to cater for ever increasing energy and other related requirements like irrigation and domestic/industrial water supplies and sometimes incompatible requirement for storage such as flood control.

Damage or failure of Dams during earthquakes have happened many times in the past such as sliding of San Feranado dam during the earthquake in 1971 (Kramer, 1996) and cracking in Koyna dam during the Koyna earthquake of December 11, 1967 (Chopra, 1996). One of the causes is the deficiency in the analysis of the effect of earthquakes. Extensive theoretical analysis have been done regarding their static behavior and various methods and codes provisions are available for the static design of dams. The static behavior of dams is generally performed on the basis of assuring reasonable factor of safety against sliding, overturn and no tension at base. The behavior of dams during earthquake loading is a complex soil-structure interaction problem involving cyclic plastic deformation and large strain. In the past it was very difficult to simulate all the phenomena that would occur during seismic loadings. Now presently, it is possible to compute various phenomena related to seismic loading such as, intensity, duration and frequency of loading. With respect to earth dams/earth and rock fill dams, the design factor are more complex. Since failure may be occasioned either by vibrations or shearing or by both. Long duration of

subsidence of foundation. These two effects will cause the crest height to be lowered in relation to reservoir level. As a consequence, over topping will cause the failure of the dam. It is also to be noted that earth dams located in the vicinity of a fault are more prone to failure by shear. Hence, due consideration is to be given to this geological aspect during the design stage.

## 4.2 CLASSIFICATION OF DAM

Dam can be classified in to different categories depending upon the purpose or basis of the classification (Punamia 1990).

### 4.2.1 According to Use

According to use dams are classified as

*(i) Storage dam* : This is the most common type of dam normally constructed. Storage dam is constructed to impound water to its upstream side during the periods of excess supply in the river and used in period of deficient supply. The storage dams may be constructed for various purposes, such as for irrigation, water power generation or for water supply for public health purposes or it may be for a multi-purpose project.

*(ii) Diversion dam* : The purpose of a diversion dam is to simply rise water level slightly in the river and thus provides head for carrying or diverting water into ditch, canals or other conveyance system to the place of use. The common examples of diversion dams are weirs and barrages.

*(iii) Detention dam* : A detention dam is constructed to store water during floods and release it gradually at a safe rate, when the flood recedes. Such detention dams also serve to spread water and thus serve as a means of artificial recharge for aquifers in the vicinity.

### 4.2.2 According to Hydraulic Design

According to hydraulic design, dams can be classified as given below.

*(i) Non-over flow dam*

In this type of dam, the top of the dam is kept at a higher elevation than the maximum expected high-flood level and water is not permitted to overtop the dam. In this discharges of excess storage water through spillways has been done.

*(ii) Over-flow dams*

In this discharge of surplus water from the reservoir flows over the crest. Hence these dams are built either of masonry or concrete.

### 4.2.3 According to Material

According to this the dams may be classified as follows :

### 4.2.3.1 Rigid dams

Those which are constructed with rigid materials such as masonry, concrete, steel or timber are known as rigid dam. Rigid dams may be further classified as follows :

    (i)     Solid masonry or concrete gravity dam

    (ii)    Arched masonry or concrete dam

    (iii)   Concrete buttress dam

    (iv)   Steel dam

    (v)    Timber dam

*(i) Gravity dams*

In the gravity dam external forces such as water pressure, wave pressure, silt pressure, uplift pressure etc. are resisted by the weight of dam itself. Thus the forces of the stability of dam are resisted by gravity forces of the mass of the dam. A gravity dam may be constructed either of masonry or of concrete.

45

*(ii)   Arched dams*

An arch dam is a dam curved in plan and carries at major part of its water load horizontally to the abutments by arch action. This part of water load depends primarily upon the amount of curvature. The balance of water load is transferred to the foundation by cantilever action.

*(iii)   Butress dams*

A buttress dam consists of a number of buttresses or piers dividing the space to be dammed in to a number of spans. To hold up water and retain the water between these buttresses panels are constructed of horizontal arches or flat slab

*(iv)   Steel dams*

Steel dams are constructed with a frame work of steel with a thin skin plate as deck slab on the upstream side.

*(v)   Timber dams*

A timber dam is constructed of frame work of timber struts and beams, with timber plank facing to resist water pressure.


## 4.2.3.2   Non-rigid dams

Non-rigid dams are those which are constructed of non-rigid materials such as earth and/or rock fill. The most common types of non-rigid dams are :

(i)   Earth dam

(ii)   Rock fill dam

(iii)   Combined earth and rock fill dam


Earth dams are made of locally available soil and gravels and therefore, most common types of dams used up to moderate heights. In earth dams the core is provided of impervious material (such as clay) upstream and down stream is

provided previous shell. For slope protection stone pitching is provided on sloping area. Filter is provided in toe downstream

A rock fill dam is an embankment which uses variable sizes of rock to provide stability and an impervious membrane to provide water tightness. We have taken earth and rock fill dam models for analysing the effect of position of source and water level in reservoir on the characteristics of the SGM.

## 4.3 SPECIFICATION OF MODELS :

In this dam simulation study, we have taken eight different cases in terms of position of source, receivers and water level in reservoir. Geometry of dam section is same in all the eight cases. Following cases has been considered in the simulation.

### 4.3.1 5.1 Full Filled Reservoir

    *(a) Source below the dam*

    (i) Receivers at MFL

    (ii) Receivers at base of reservoir

    *(b) Source at off-set*

    (i) Receivers at MFL

    (ii) Receivers at base of reservoir

### 4.3.2 Half Filled Reservoir

    *(a) Source below the dam*

    (i) Receivers at MFL

    (ii) Receivers at base of reservoir

    *(b) Source at off-set*

    (i) Receivers at MFL

    (ii) Receivers at base of reservoir

The dam geometry and different positions of source and receivers have been shown in Fig.4.1. The depth of dam in 325m and thickness of soil sediment is 25m and 50m free board. Similarly, the areal extent at top of dam in 3500m and base in 400m wide. Source has been placed at a depth of 9850 m from the surface. First position of source is 2750 m from left edge and second position of source is at 5250 m offset from first position of source. The parameters of the different layers of the dam model which are same for all eight models, have been given in table 4.1. Ten receivers have been placed in each model at an equal spacing of 500 m. The computer program has been modified according to dam geometry. The model parameter listed in Table 4.1, have been assigned to each grid point. Then dip slip source, based on partial stress drop has been implemented into the computational grid at the desired positions. The following computational parameters have been taken in the simulations. These model parameters fulfill the requirement to make the simulation stable and dispersion free.

**Model Specification**

Model size in term of grid        :  400 (H) x 450 (V) grid

Time step                         :  0.0015 second

Maximum time                      :  12 second

Total No. of time steps           :  8000

Dominant frequency                :  5 Hz

Type of source                    :  Dip-Slip

We get the particle displacement registered by ten receivers after running the computer program. The graph of particle displacement (cm) $V_s$ time (second), at different receivers have been drawn.
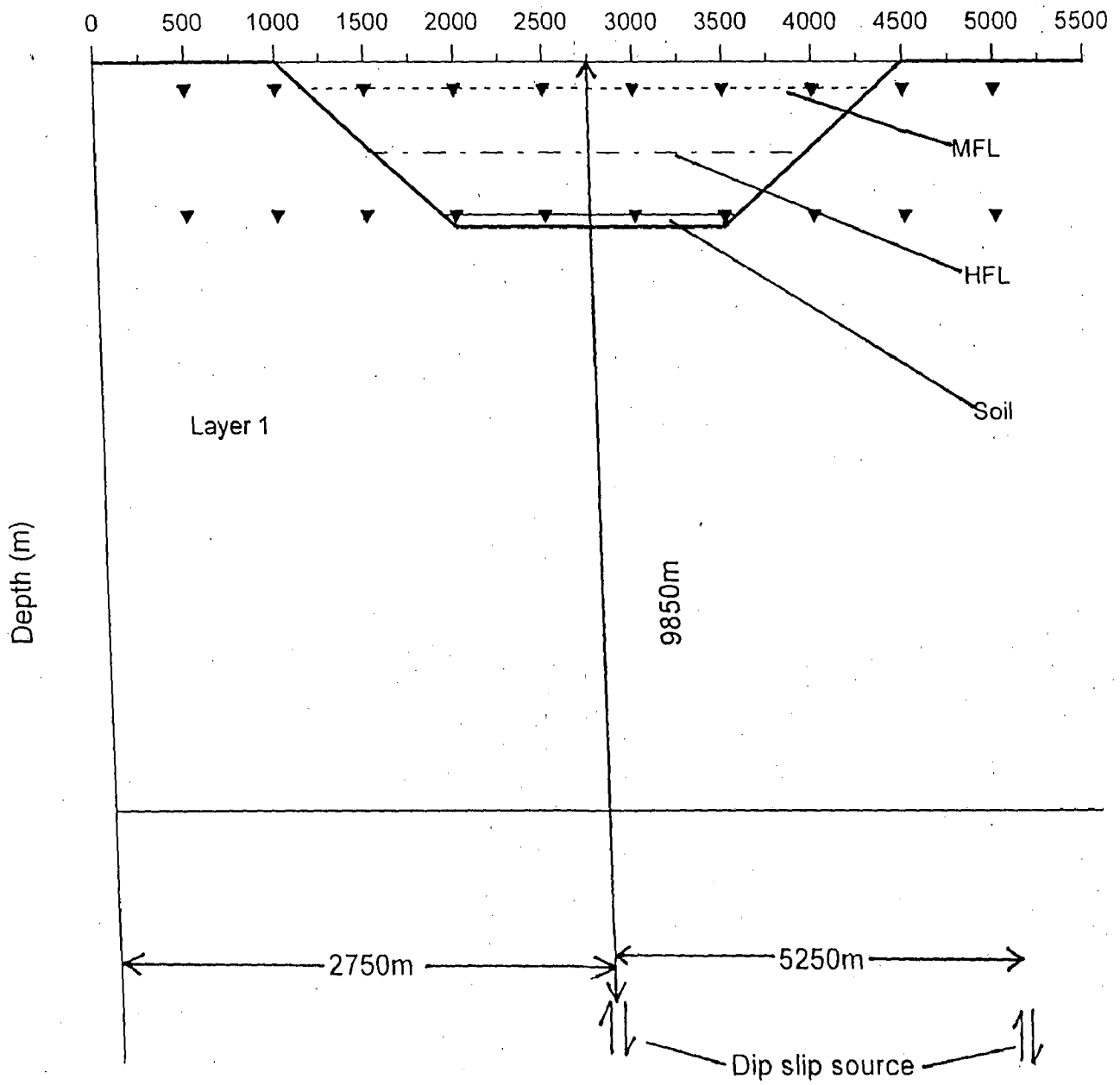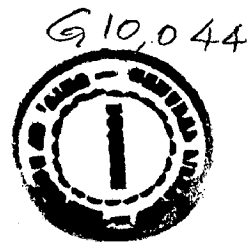
Fig. 4.1 Model geometry of dam

**Table 4.1 Layer Parameters of the Geological Model**

| S.NO. | LAYER NUMBER | THICKNESS (M) | MATERIAL DENSITY ($\rho$) (G/CC) | SHEAR WAVE VELOCITY ($V_S$) (M/S) | RIGIDITY $\mu$(N/M$^2$) |
|---|---|---|---|---|---|
| 1 | WATER | VARIABLE | 1.02 | 0 | 50 |
| 2 | SOIL | 25 | 1.70 | 500 | $0.425 \times 10^6$ |
| 3 | LAYER I | 7500 | 2.50 | 2500 | $15.625 \times 10^6$ |
| 4 | LAYER II | -- | 2.70 | 2598.07 | $18.224 \times 10^6$ |

50

G 10,044.

## 4.4 NATURE OF GRAPHS WHEN RESERVOIR IS FULL

### 4.4.1 Source Below the Dam

*(A)  Receivers at top of water surface*

The following observations have been drawn from the numerical response as shown in Fig.4.2.

(1)  · The amplitude of particle displacement recorded by receiver number 8 from left is maximum.

(2)  The amplitude of particle displacement recorded by receiver number 3 to 7 placed on water surface is zero since shear wave can not move in water.

(3)  The signals obtained after '9' second are multiple reflections between the base of dam and base of first layer.  Duration of these multiples is due to leakage of energy from the soil at the base of dam at different reflections from the base of the soil.

(4)  Amplitude is decreasing with offset.

*(B)  Receiver at base of reservoir*

The following observations have been drawn from the numerical response as shown in Fig.4.3.

1.  Maximum amplitude and duration of particle displacement is recorded by receiver number 4 to 7, which are placed at bottom of reservoir.  This maximum amplitude of particle displacement is due to amplitude amplification in soil and multiple reflection and numerical dispersion of waves in soil.  This numerical dispersion is due to very small velocity of wave in soil.  Effectively there are only four grid per wave length whereas the minimum number of grids required per wave length is 10 to avoid the numerical grid dispersion.
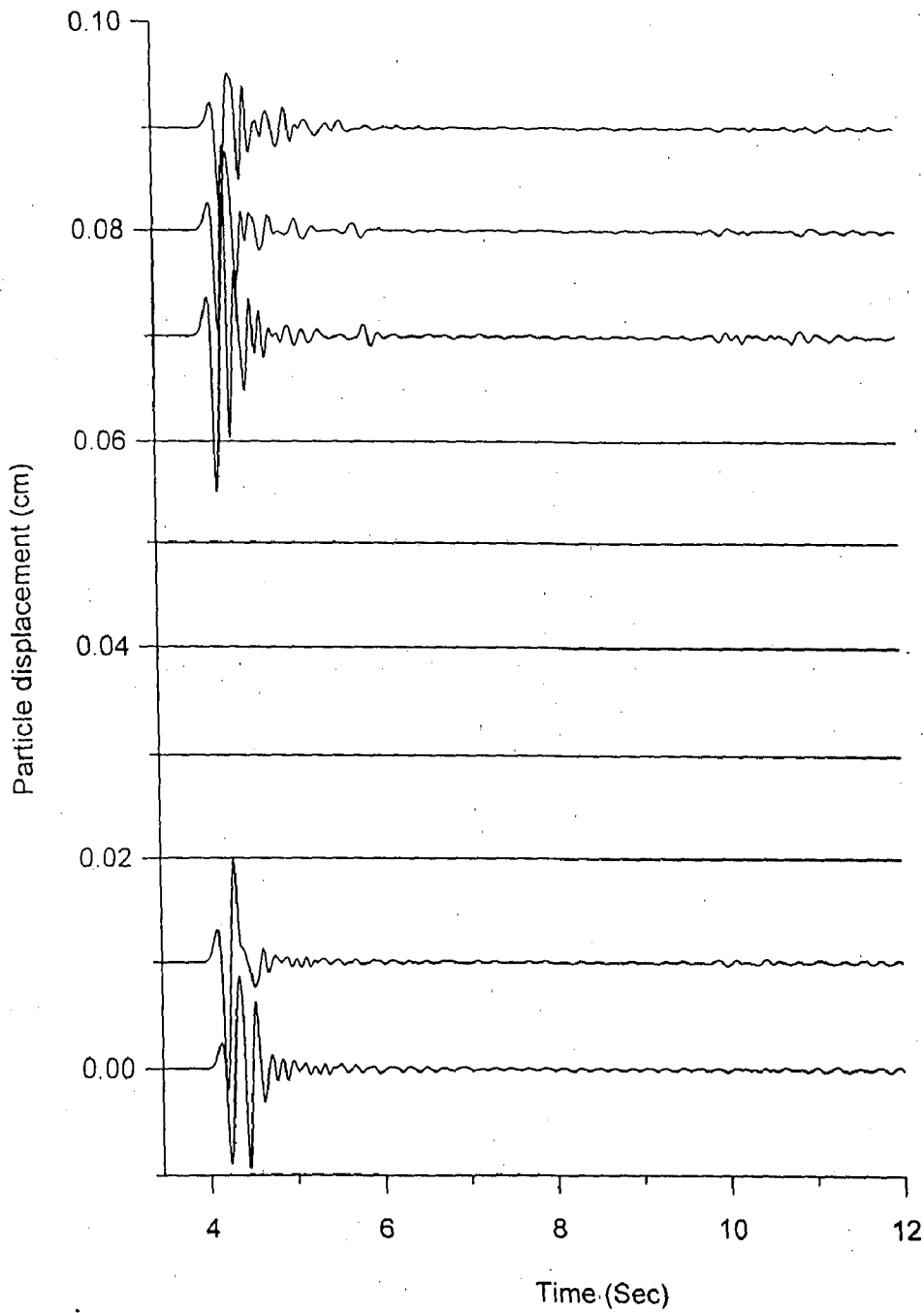
51

Fig 4.2 Response of full filled reservoir for Dip-Slip source below
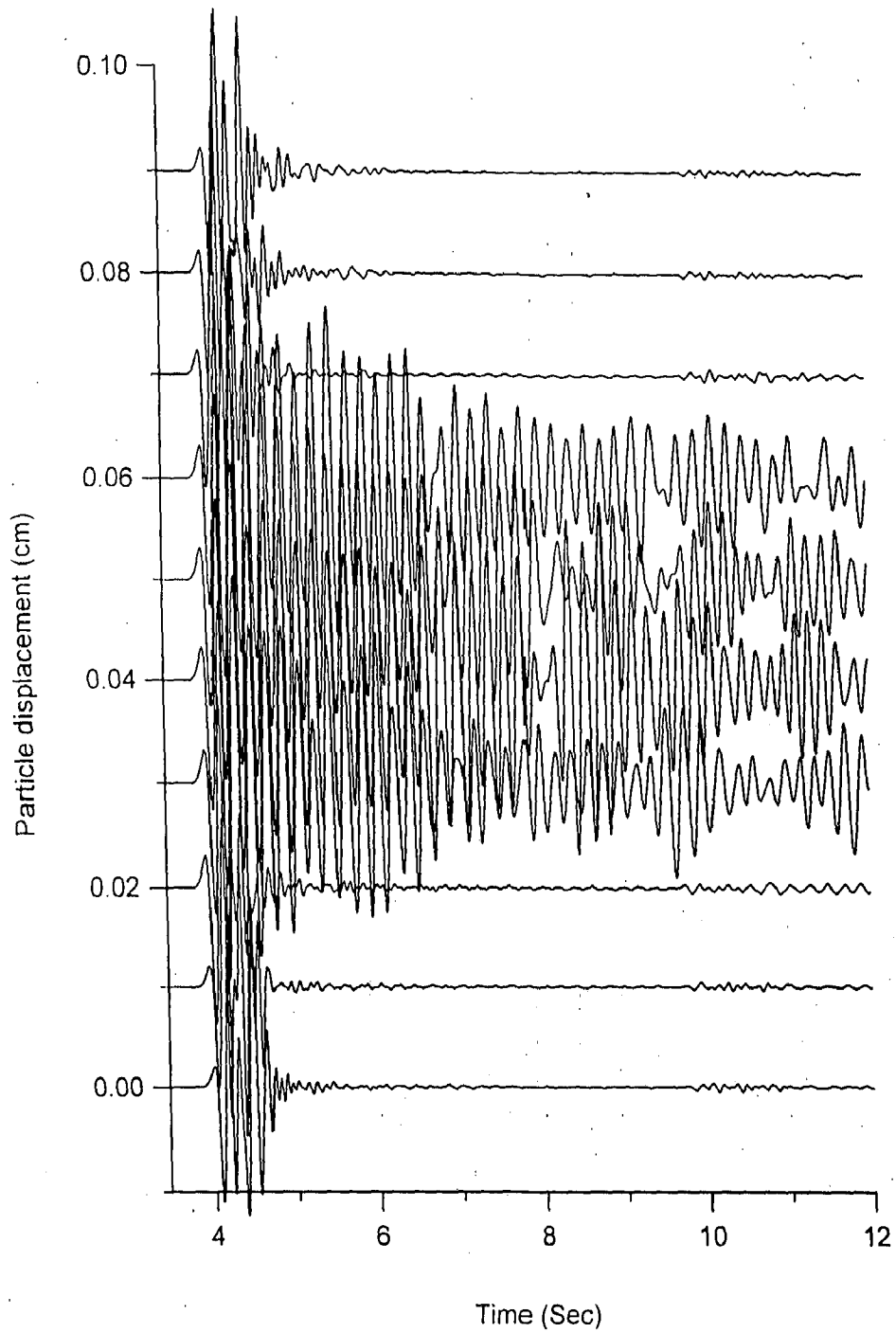the reservoir and receivers at the surface of water level

Fig 4.3 Response of full filled reservoir for Dip-Slip source below
the reservoir and receivers at the base of reservoir

53

2. The signal obtained after 9 second are multiple reflection between base of dam and base of first layer. Duration of signal are due to leakage of energy from the soil due to multiples

3. Arrival time of signal at different receiver positions are in agreement with the model geometry and position of source.

## 4.4.2 Source at off-set

*(A) Receivers at top of water surface*

The following observations have been drawn from the numerical response as shown in Fig.4.4.

1. The amplitude of particle displacement recorded by receiver number 8 from left is maximum.

2. The amplitude of particle displacement recorded by receiver number 3 to 7 placed on water surface is zero since shear wave can not move in water.

3. The amplitude of particle displacement recorded by receiver number 10 from left is greater than receiver number 1 since receiver number 10 is nearest to the source.

4. Arrival time is increasing from receiver number 10 to 1 due to increase of distance from the source.

*(B) When receivers at base of reservoir*

The following observation has been drawn from the numerical response as shown in Fig.4.5.

1. Amplitude and duration at receiver number 1, 2, 3 is lesser than receiver number 8, 9, 10.

2. The signal obtained after 9 second are multiple reflection between base of dam and base of first layer. Duration of signal are due to
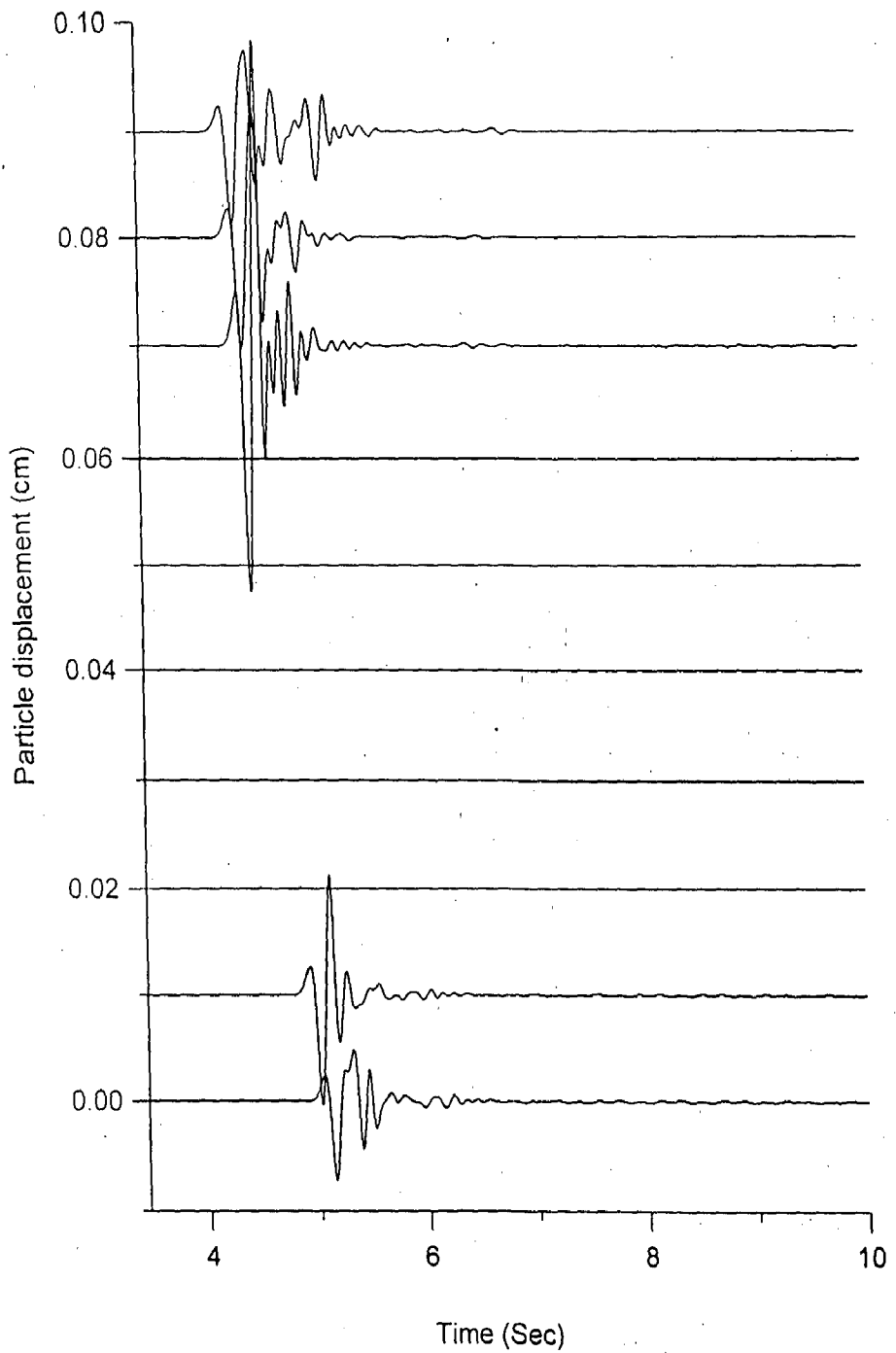
Fig 4.4 Response of full filled reservoir for Dip-Slip source at offset
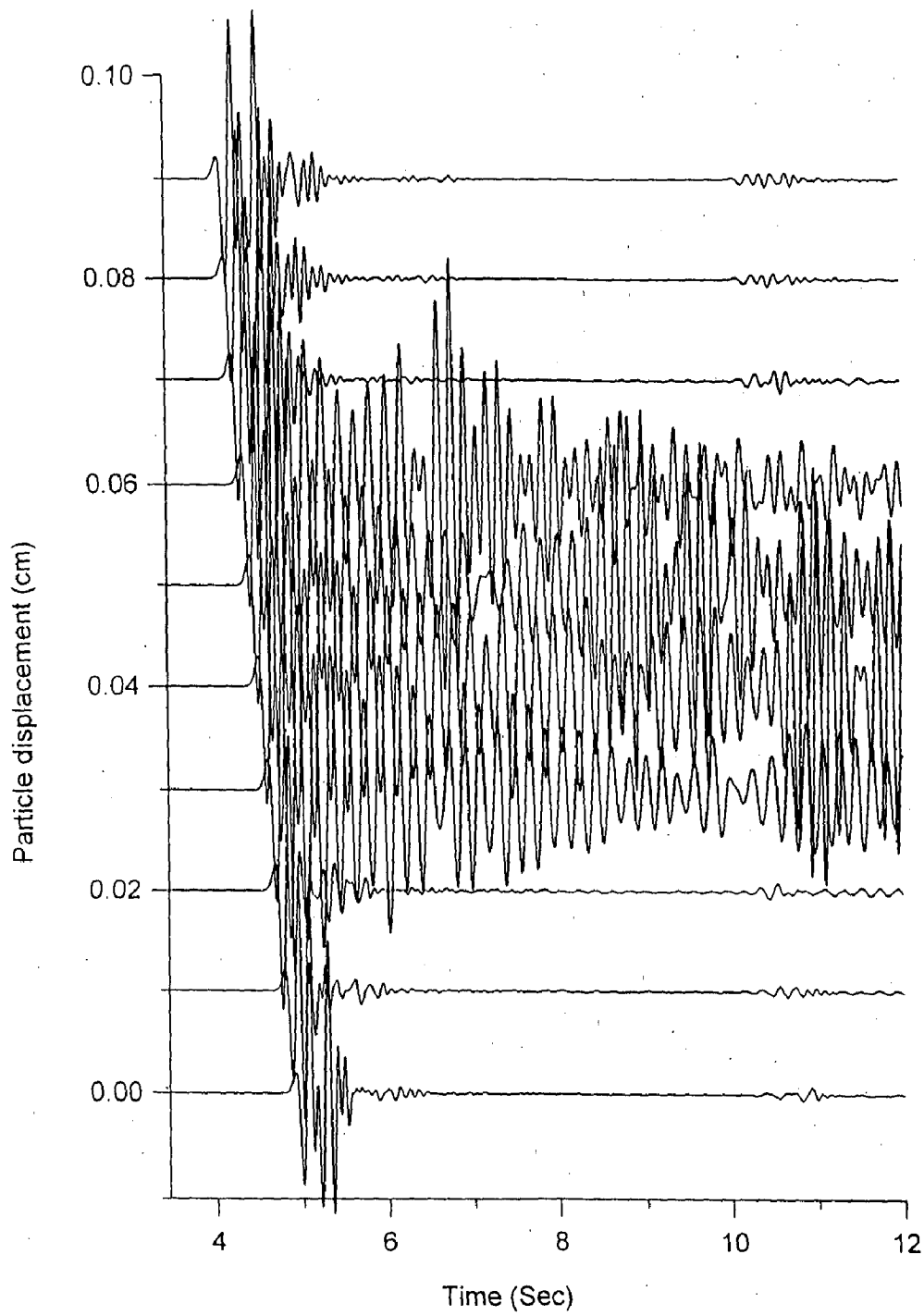and receivers at the surface of water level

Fig 4.5 Response of full filled reservoir for Dip-Slip source at offset
and receivers at the base of reservoir

leakage of energy from the soil.

3. Maximum amplitude of particle displacement is recorded by receiver number 4 to 7, which is placed at bottom of reservoir due to amplification in soil.

4. Receiver number 10 recorded more amplitude in comparison to receiver number 1. since receiver number 10 is nearer to source.

## 4.5 EXPLANATION OF GRAPHS WHEN RESERVOIR HALF FILLED

### 4.5.1. Source Below the Dam

*(A) Receiver at top of water surface*

The following observation has been drawn from the numerical response as shown in Fig.4.6.

1. Maximum amplitude of particle displacement is recorded by receiver number 2 from left.

2. The amplitude of particle displacement recorded by receiver number 3 to 8 placed on water surface is zero. Since shear wave velocity in water is zero.

3. Four receivers 1, 2 and 9, 10 show some amplitude of particle displacements after the attainment of maximum amplitude, but we see that the amplitude of these later stage recordings is more dominant in case of receiver number 1 and 2.

*(B) When receiver at base of reservoir*

The following observation has been drawn from the numerical response as shown in Fig.4.7.

1. Maximum amplitude of particle displacement is recorded by receiver number 4 to 7, which is placed at bottom of reservoir. Explanation of this, is same as previous case (4.6.1b).
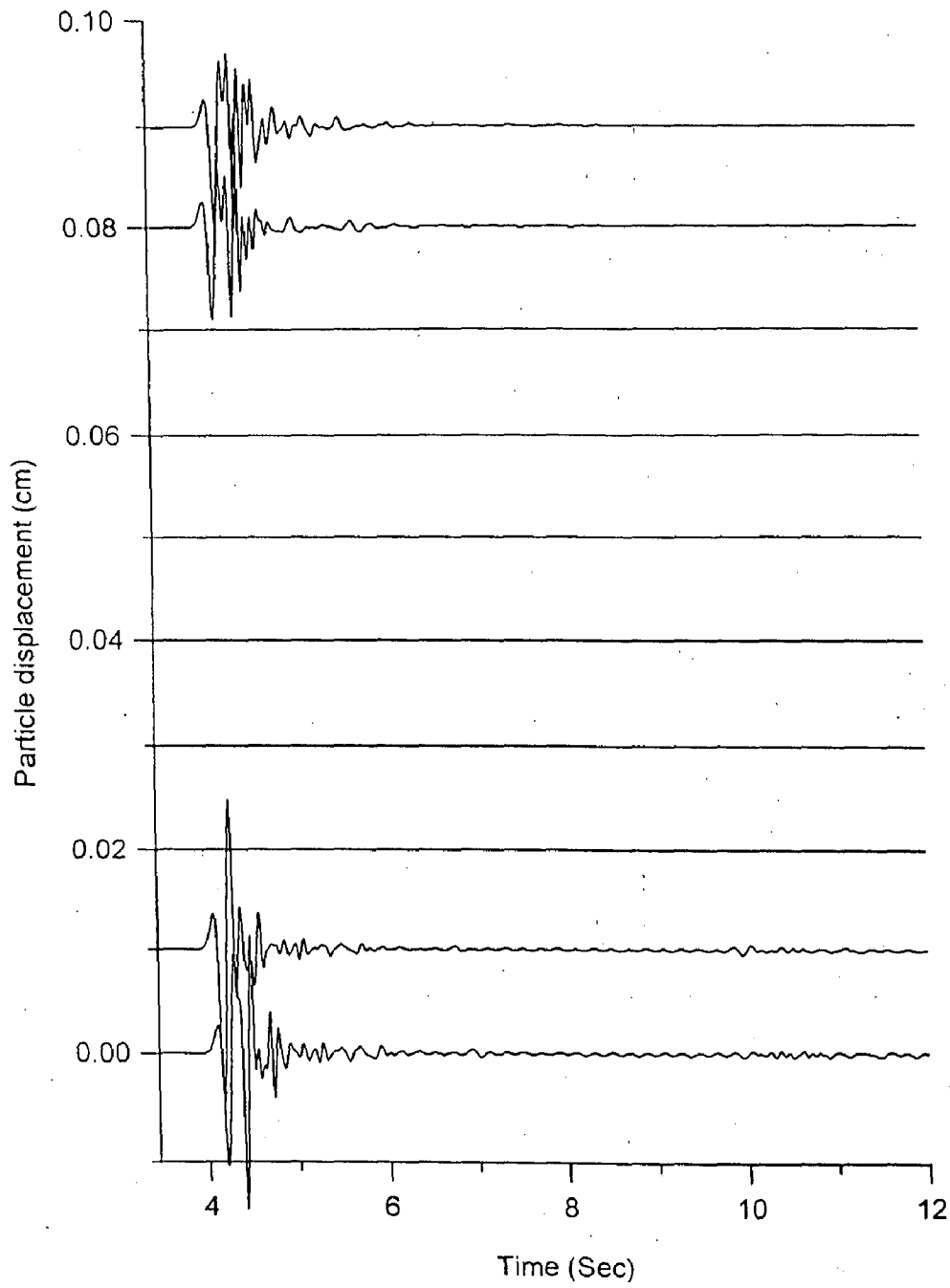
Fig. 4.6 Response of half filled reservoir for Dip-Slip source below the reservoir and receivers at the surface of water level
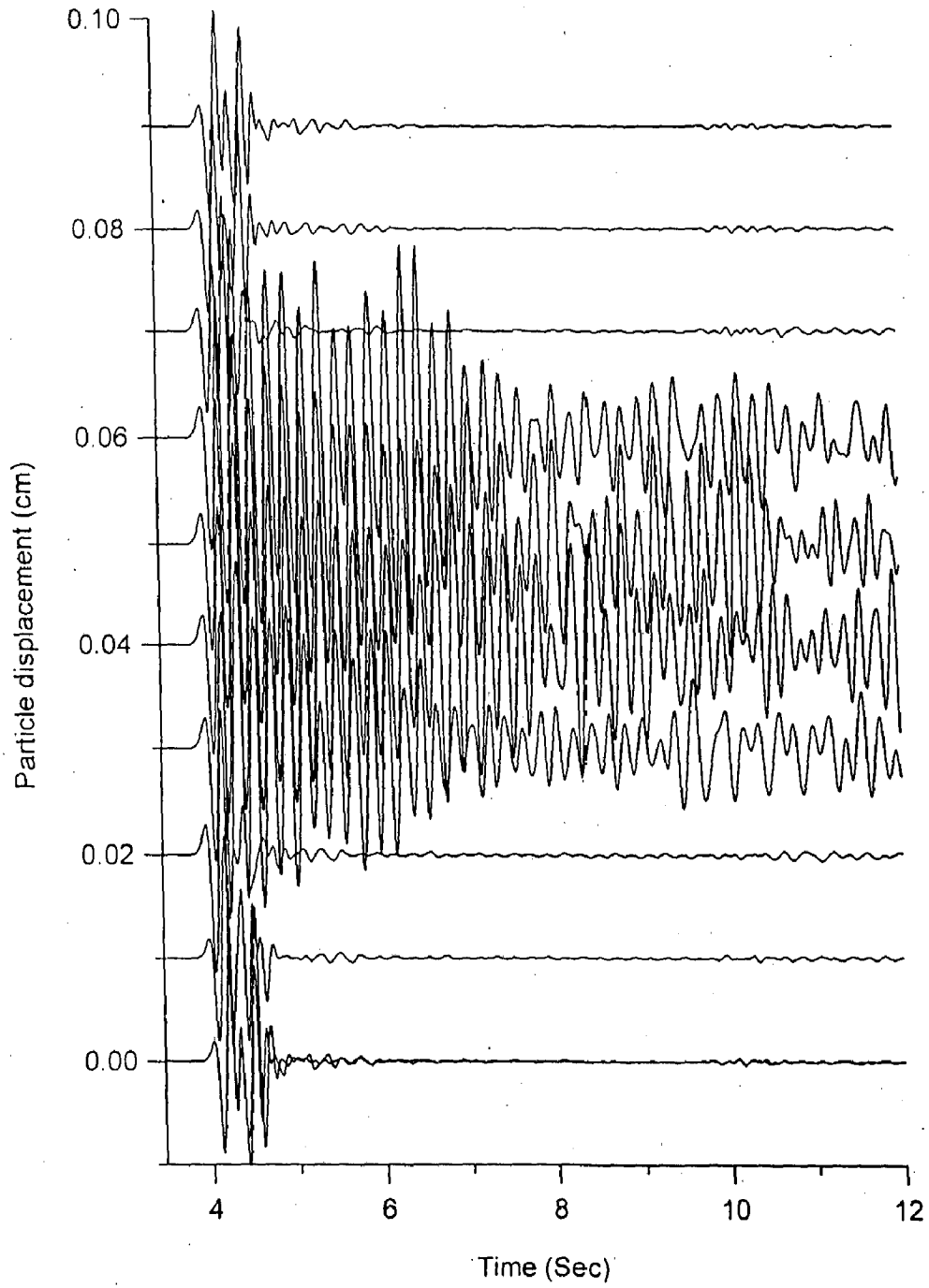
Fig. 4.7 Response of half filled reservoir for Dip-Slip source below the reservoir and receivers at the base of reservoir

59

2. Maximum amplitude recorded by receiver number 1 and 10 is almost same due to same distance from source.

3. Other visible effects are same as mentioned in previous cases.

### 4.5.2 Source at offset

*(A) Receivers at top of water surface*

The following observation has been drawn from the numerical response as shown in Fig.4.8.

1. Maximum amplitude of particle displacement recorded by receiver number 2.

2. Shear wave velocity in water body is zero. Hence receiver number 3 to 8 have no response.

3. Other visible effects are same as mentioned in previous case.

*(B) Receiver at base of reservoir*

The following observation has been drawn from the numerical response as shown in Fig.4.9.

1. In this case also maximum amplitude of particle displacement is recorded by receiver number 4 to 7.

2. Arrival time of signal is maximum at receiver number 1 and minimum at receiver number 10, due to position of receivers with respect to source.

3. In this case amplitude of signal after 9 second is more as compared with the previous cases.

4. Other visible effects are same as mentioned in previous case.

The two layer model excluding dam was also simulated using sources positions as in the previous case, keeping reaches at the surface only the computed responses have been shown in Figs 10 and 11 four two source positions. The

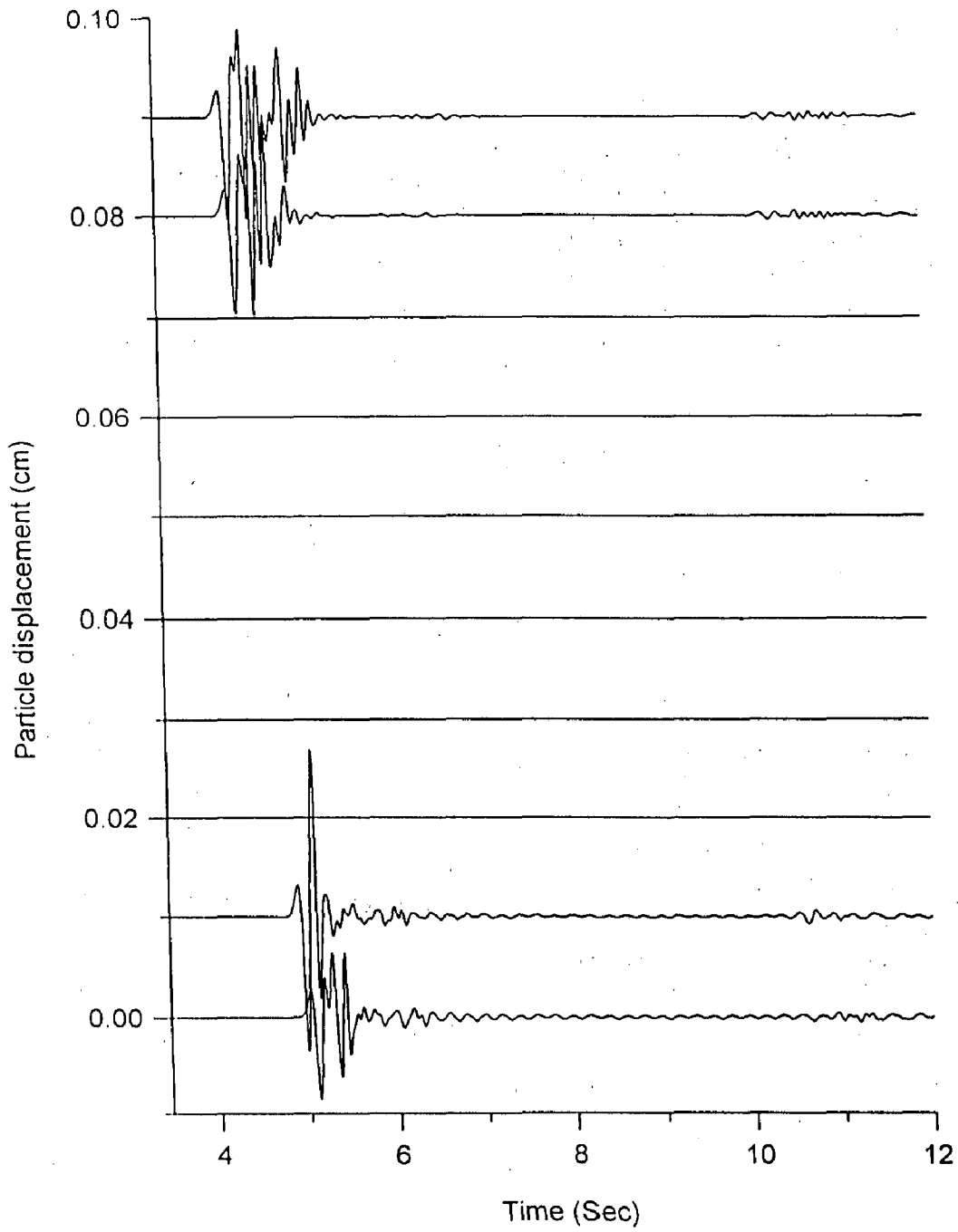Fig. 4.8 Response of half filled reservoir for Dip-Slip source at offset
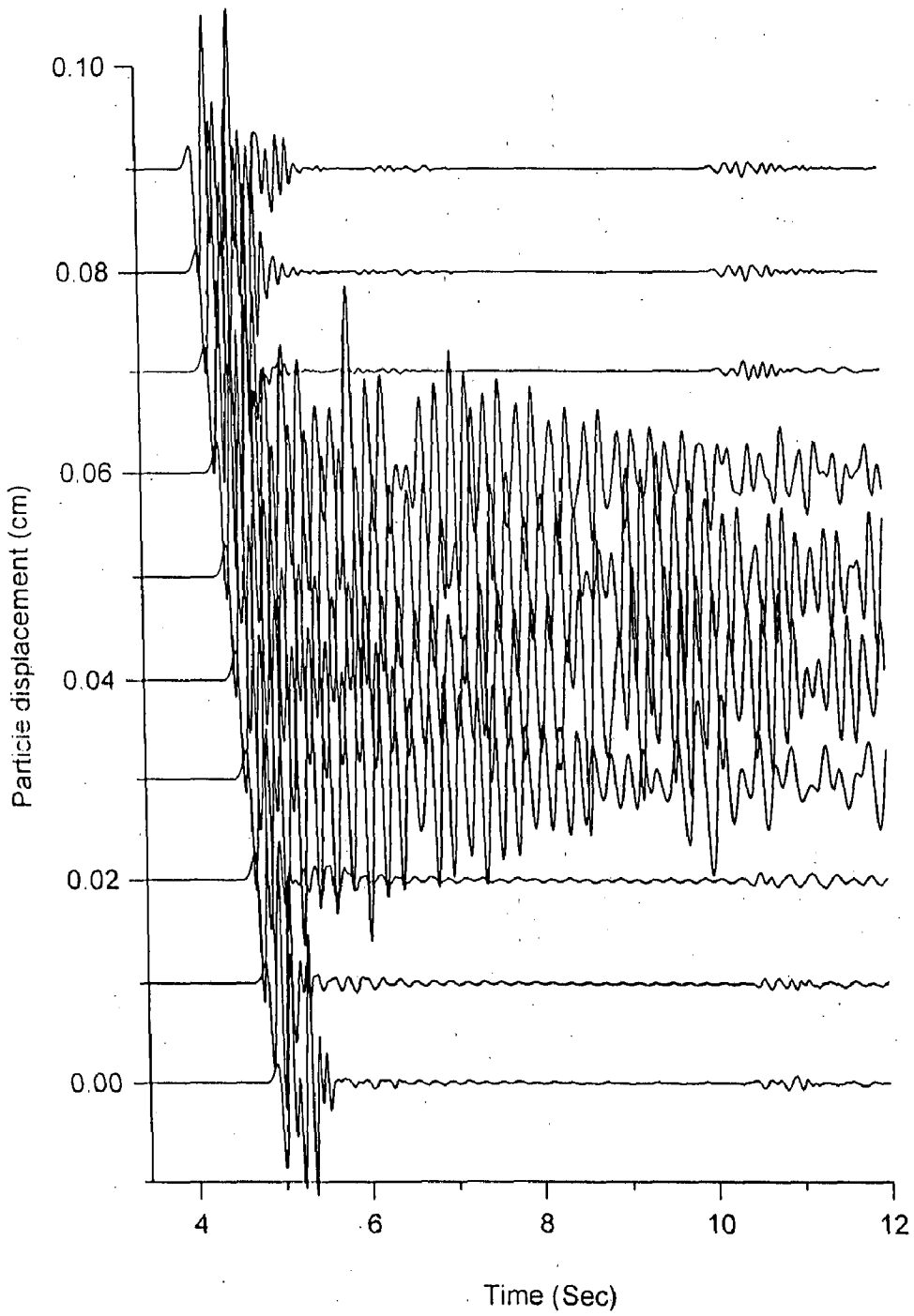and receivers at the surface of water level

Fig. 4.9 Response of half filled reservoir for Dip-Slip source at offset
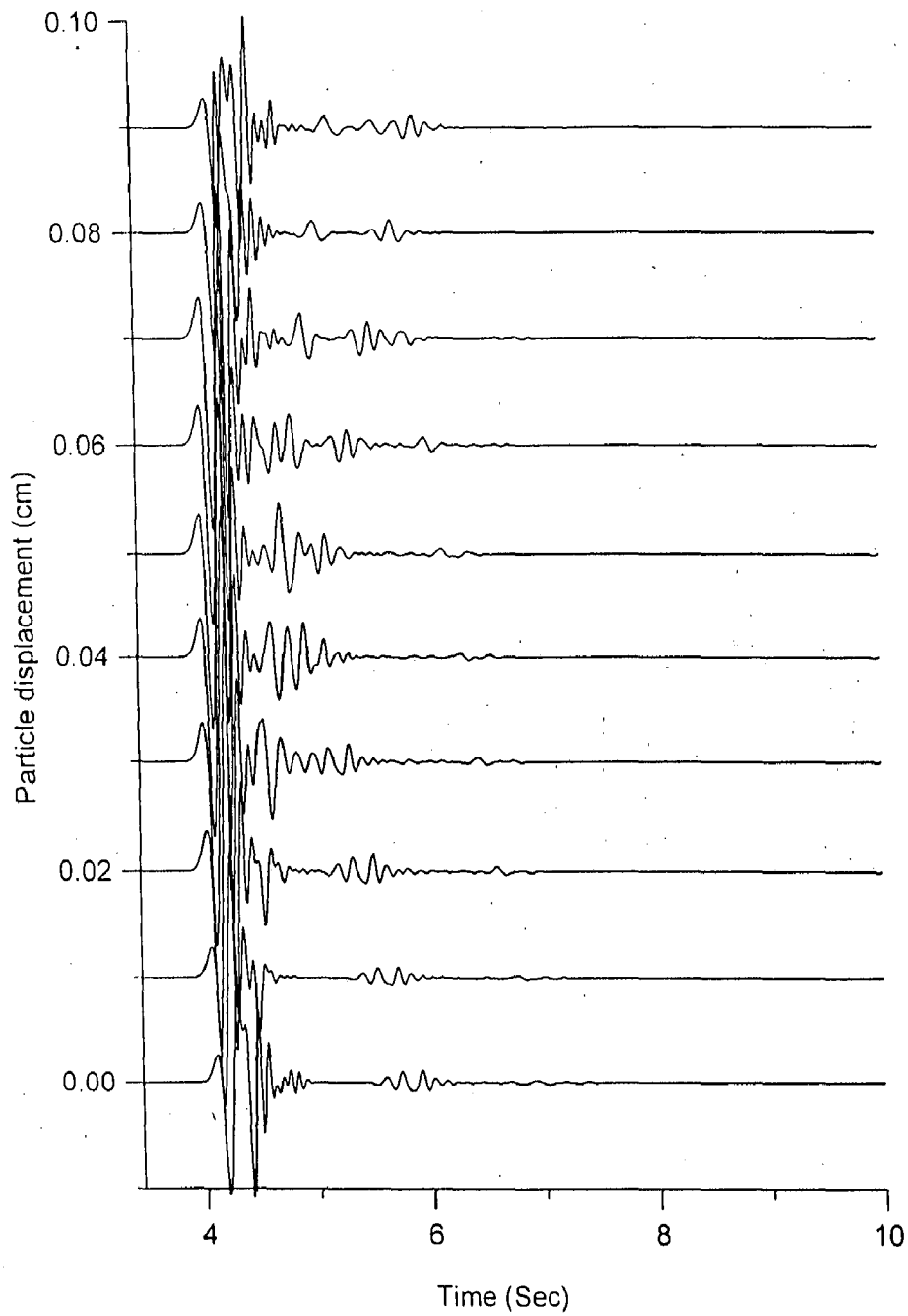and receivers at the base of reservoir

Fig. 4.10 Response of tow layer model (excluding dam) when source
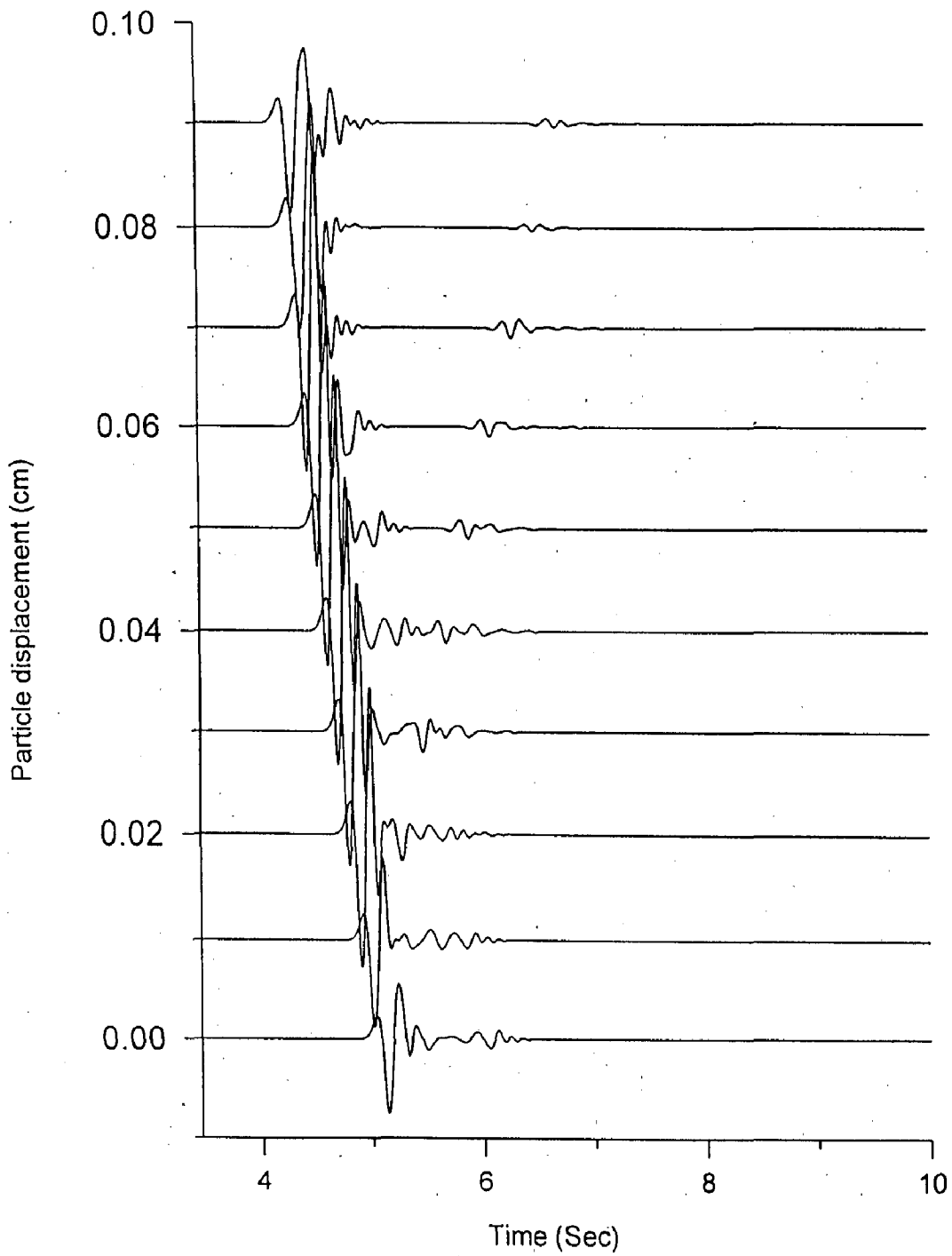is below the spread

63

Fig. 4.11 Response of tow layer model (excluding dam) when source
is at an off set of the spread

critical examination of these and all the other responses for dam illustrates that the presence of dam causes considerable change in the characteristics of the SGM.

## 4.6 EFFECT OF HEIGHT OF WATER IN RESERVOIR

The following conclusions has been drawn from the numerical responses.

1. There is increase of amplitude and duration at the surface receivers when reservoir is half filled as compared to when the reservoir was full filled.

2. But, there is reverse effect at the base of the dam i.e. both amplitude and duration are smaller when reservoir is half filled as compared to the response when reservoir was full filled.

## 4.7 EFFECT OF SOURCE POSITION

The following conclusions has been drawn from the numerical responses.

1. There is tremendous increase of amplitude and duration at receiver number 7 when source is at an offset of 5250 m from the centre of the spread. This effect may be due to the focusing of energy.

2. The amplitude of signal after 9 second is more at receiver number 1 and 2 due to directivity effects in the offset cases.

Indian subcontinent is one of the most seismically active regions of the world. Seven catastrophic earthquake of magnitude ≥8.0 have caused great loss of human lives, property and engineered structures. The high frequency strong ground motion (SGM) is least understood area due to lack of strong motion data. Numerical methods can be used to find out the SGM characteristics (amplitude frequency and duration) for earthquake resistant design, taking the available geological and seismicity data into consideration. Parsimonious staggered grid approximation of elastodynamic equation for SH wave has been done by J.P. Narayan (1998) using the staggering technique of Luo and Schuster, (1990) and an algorithm has been developed. Numerical seismic sources based on shear dislocation (Coutant et al., 1995); such as dip-slip, strike-slip or explosive sources have been implemented into the numerical grid. Numerical radiation patterns for different dislocation sources have been computed by J.P. Narayan (1998) and were found in good agreement with the analytical radiation patterns. Local site effects on SGM characteristics have been studied in detail, Boundary conditions based on Clayton and Engqusrst (1980) as well as transmissive Sponge boundaries have been applied to avoid the edge reflections.

We have studied the effect of change of slip ($U$); rupture area, stress drop ($\Delta\sigma$) and time step ($\Delta t$); on the characteristics of ground motion for the purpose of numerical source scaling. Following conclusions have been drawn from the computed results.

1.   The amplitude of particle displacement and duration is decreasing with decrease of the rupture area

2. The amplitude of particle displacement is decreasing with decrease of slip at the fault planes.

3. The amplitude of particle displacement and stresses components are increasing with stress drop.

4. The duration of particle displacement is independent of the magnitude of the stress drop.

5. There is no change in particle displacement due to variable time steps, taken in the computations.

Finally, it has been concluded that magnitude of input source can be increased by increasing either rupture area or stress drop and rupture area both but not by only increasing stress drop, since it can not explain the usual increase of duration with magnitude.

The following conclusions have been drawn from the simulated results for different geometry of the basins included in a six layered geological model.

1. Comparative study of responses of with and without basins reveals that lower shear strength in the soil facilitates amplitude amplification and increase in duration. This result corroborates with the findings of Vidale, et.al., (1988). Duration is increasing in the basin due to multiple reflection of signal in the basins.

2. The duration of signal is increasing with increase of depth of the basin.

3. The amplitude amplification and duration is more when depth of basin is more due to focusing effects.

4. Further, comparative study of responses of narrow basins and wide basins reveals that narrower and deeper the basin more will be

amplification due to further increase of focusing effects.

The following conclusions have been drawn from the simulated results for dam model with variation of source receiver positions and water level in the reservoir.

(i)   The amplitude and duration at the surface is more when reservoir is half filled as compared with the full filled reservoir.

(ii)  But, reverse effect at the base of the reservoir is obtained i.e. both amplitude and duration is smaller in the case of half filled reservoir as compared with the full filled reservoir.

(iii) There will be tremendous increase of amplitude and duration at that side at which wave is reaching first, due to the focusing. This effect will very much depend on the focal depth, epicentral distance and the size of the dam.

(iv)  The amplitude and duration of particle displacement at the base of the dam is very hight due to soil amplification. The duration of particle displacement has been further amplified due to the numerical grid dispersion.

Simulated results for different source parameters, basin geometry and dam models reveals that now realistic source can be generated and SGM characteristics can be predicted by taking into account the crustal path and local site conditions for a particular seismically active region. This type of study will be most useful in rick analysis and preparing for the impending earthquake in an area where there are no ground motion records.

# REFERENCES

♦ Anderson, J.G., Bodin, P., Brune, J.N., Prince, J., Singh, S.K., Quaas, R. and Onate, M. (1986) Strong ground motion from the Michoacan, Mexico, earthquake, Science, 233, 1043-1049.

♦ Archuleta, R.J. (1986) Downhole recording of seismic radiation. In Earthquake source Mechanics (S. Das, J. Boatwright, and C H scholz, eds.), Maurice Ewing, 6, pp. 319-329, Am. Geophys. Union, Washington, D C

♦ Bard, P.Y. and Bouchon, M. (1980a) The seismic response of sediment filled valleys, Part 1. The case of incident SH-waves, BSSA, 70, 1263-1286.

♦ Brune, J.N. (1970) Tectonic stress and spectra of seismic shear waves from earthquakes, J. Geophys. Res., 75, 4997-5009

♦ Boatwright, J. (1980), A spectral theory for circular seismic source : Simple estimates of source dimension, dynamic stress drop, and radiated seismic energy. . 70, 1-27.

♦ Clayton, R.W. and Engquist, B. (1980), Absorbing side boundary conditions for wave equation migration, Geophysics, 45, 895-904.

♦ Coutant, O, Virieux, J. and Zollo, A. (1995) Numerical source implementation in a 2D finite difference scheme for wave propagation, BSSA, 85, 1507-1512.

♦ Chopara, A.K. (1996) Dynamics of structures Prentic Hall , New Jersey, U.S.A.

♦ De Mets, C. Gordon , R.G., Stein, S., and Argus, D.F. (1987) A revised estimate of pacific North America motion and amplifications for western North America plate boundary tectonic , Geophys . Re. Lett, 14,: 911-14.

▶ Dimitriu, P.P., Papaioannaou, C.A. and Theodulidis, N.P. (1998) EURO-SEISTEST strong motion array Thessaloniki, Northern Greece, A study of site effects, BSSA, 88, 862-873.

▶ Dobr, R. and Vuectic, M. (1987) Dynamic properties and seismic response of soft clay deposits. Proceedings, International Symposium on Geotechnical Engineering of soft soils, Mexico City, 2, . 51-87.

- Frankel, A., and Wennerberg, L. (1989). Microeathquake spectra from the Anza, Califorina, seismic network :Site response and source scaling, BSSA, . 79, . 581-609.

- Gutenberg, B. (1927) Grundlagen der Erdlebenkunde, Berlin.

- Glassmoyer, G. and Borcherdt, R.D. (1990) Source parameters and effects of bandwidth and local geology on high-frequency ground motions observed for aftershocks of the north-eastern Ohio earthquake of 31 January 1986, BSSA,.80, 889-912.

- Hanks, T.C. and McGuire, R.K.(1981).The character of high frequency strong ground motion. BSSA, . 71..2071-2095.

- Hanks ,T.C. and Johnson , D.A. (1976), Geophysical assessment of peak accelerations. 66, 959-68.

- Kanamori, H. and Anderson, D.L.(1975) Theoretical basis of some empirical relations in seismology, BSSA, 65,. 1073-1096.

- Kelly, K.R., Ward, R.W., Trietel S. and Alford, R.M. (1976) Synthetic seismograms: A finite difference approach, Geophysics, 41, 2-27.

- King. J.L. and Tucker. B.E.(1984). Dependence of sediment-filled valley response on the input amplitude and the valley properties, BSSA, 74, 153-165.

- Kramer, S.L.,(1996), geotechnical Earthquake Engineering, Prentice Hall, New Jersey, U S A

- Luco, J. E., and Anderson, J. G. (1983) Steady- state response of an elastic half-space to a moving dislocation of finite width ,BSSA 73, 1-22.

- Luo,Y. and Schuster, G. (1990), Parsimonious Staggered Grid Finite Differencing of the Wave equation, Geophys. Res. Lett., 17, 155-158.

- Punamia, B. C. and Lal, B.B. (1990) Irrigation and water power engineering.(1990),Standard Publication , New Delhi.

- Macmurdo, J.(1824) Papers relating to the earthquake which occurred in India in 1819 Philosophical Magazine, 63. 105-177.

- Mallet, R.(1862). Great Neapolitan Earthquake of 1857, London.

◆ McGarr, A. (1986) Some observation indicating complications in the nature of earthquake scaling. In "Earthquake source mechanics" (S. Das, j. Boatwright, and C. H. Scholz, eds.),Maurice Ewing, 6, 217-225, Am. Geophys. Union, Washington, D. C.

◆ Narayan, J. P. and Ram, A. (1998) Simulation of geological structures using SH-wave solution, Acta Geophy. Polonica,XLVI 115-126.

◆ Narayan, J. P.(1998) Numerical strong ground motion simulation and study of local site effects, Proceedings of the 11th 'Symposium on Earthquake Engineering', in the Department of Earthquake Engineering, UOR, Roorkee, December 17-19,

◆ Rai, D. C., Narayan, J. P., Pankaj and Kumar,A (1997) Jabalpur earthquake of May 22, 1997, Reconnaissance report. Department of Earthquake Engineering, University of Roorkee, Roorkee.

◆ Reid, H.F. (1910), The California Earthquake of April 18,1906, Publication 87, 21. Carnegin Institute of Washington, Washington, D. C.

◆ U.S. Geological Survey Staff (1990) The Loma Prieta , california earthquake: an anticipated event, Science, 247, 286-293.

◆ Vidale, J.E., Helmberger, D.V. and Clayton, R.W (1985) Finite difference seismograms for SH-waves, BSSA, 75, 1765-1782.

◆ Vidale, J.E. and Helmberger, D.V. (1987) Path effect in strong motion seismology. In "Seismic Strong Motion Synthetics" (Bolt, B.A., ed.), Academic Press, Orlando, Fla.

◆ Vidale, J.E. and Helmberger, D.V. (1988) Elastic finite difference simulation of the 1971 San Fernando earthquake, BSSA, 78, 122-141.

◆ Virieux, J. (1984) SH-wave propagation in heterogeneous media, velocity stress finite-difference method, Geophysics, 49, 1933-1957.

◆ Wood, H . O. (1908).Distribution of apparent intensity in San Francisco, in the California earthquake of April 18,1906, Report of the state. Earthquake investigation commission, Carnegie institute of Washington, Washington, D.C., 220-245.